Nov. 20, 2000 Submitted to JGR Oceans
Revised July 17, 2001

Variability of Antarctic Sea Ice 1979-1998

H. Jay Zwally, Josefino C. Comiso, Claire L. Parkinson, Donald J. Cavalieri and Per Gloersen

Oceans and Ice Branch, Code 971, NASA/Goddard Space Flight Center

Variability of Antarctic Sea Ice 1979-1998

H. Jay Zwally, Josefino C. Comiso, Claire L. Parkinson, Donald J. Cavalieri and Per Gloersen
Oceans and Ice Branch, Code 971, NASA/Goddard Space Flight Center

ABSTRACT

The principal characteristics of the variability of Antarctic sea ice cover as previously described from satellite passive-microwave observations are also evident in a systematically-calibrated and analyzed data set for 20.2 years (1979 -1998). The total Antarctic sea ice extent (concentration >15%) increased by 13,440 ± 4180 km^2/year (+1.18 ± 0.37%/decade). The area of sea ice within the extent boundary increased by 16,960 ± 3,840 km^2/year (+1.96 ± 0.44%/decade). Regionally, the trends in extent are positive in the Weddell Sea (1.5 ± 0.9%/decade), Pacific Ocean (2.4 ± 1.4%/decade), and Ross (6.9 ± 1.1%/decade) sectors, slightly negative in the Indian Ocean (-1.5 ± 1.8%/decade, and strongly negative in the Bellingshausen-Amundsen Seas sector (-9.5 ± 1.5%/decade). For the entire ice pack, small ice increases occur in all seasons with the largest increase during autumn. On a regional basis, the trends differ season to season. During summer and fall, the trends are positive or near zero in all sectors except the Bellingshausen-Amundsen Seas sector. During winter and spring, the trends are negative or near zero in all sectors except the Ross Sea, which has positive trends in all seasons. Components of interannual variability with periods of about 3 to 5 years are regionally large, but tend to counterbalance each other in the total ice pack. The interannual variability of the annual mean sea-ice extent is only 1.6% overall, compared to 5% to 9% in each of five regional sectors. Analysis of the relation between regional sea ice extents and spatially-averaged surface temperatures over the ice pack gives an overall sensitivity between winter ice cover and temperature of - 0.7% change in sea ice extent per K. For summer, some regional ice extents vary positively with temperature and others negatively. The observed increase in Antarctic sea ice cover is counter to the observed decreases in the Arctic. It is also qualitatively consistent with the counterintuitive prediction of a global atmospheric-ocean model of increasing sea ice around Antarctica with climate warming due to the stabilizing effects of increased snowfall on the Southern Ocean.

1. Introduction

In recent decades, the Antarctic sea ice cover has varied significantly from year-to-year with some anomalies persisting for periods of 3 to 5 years [e.g., Zwally et al., 1983a]. However, decadal-scale sea ice changes have been smaller and more difficult to ascertain with statistical significance. Furthermore, while the physical processes (ice-ocean-atmosphere-solar) that control the annual growth and decay of sea ice are well known, the manner in which these processes combine on decadal-time scales and regional-spatial scales is complex and not well determined. In particular, the interaction of the Antarctic sea ice cover with global climate change is uncertain. In one view, the intuitive expectation that a smaller sea ice cover should be associated with warmer atmospheric temperatures is supported by some observations and models. For example, Gordon and O'Farrell [1997] modeled a decreasing Antarctic sea ice cover in a warmer climate, but with a smaller rate of decrease than their modeled rate of decrease for the Arctic sea ice. Observationally, Jacka and Budd [1991] and Weatherly et al. [1991] also showed the expected negative correlation between regional-scale sea ice changes and Antarctic coastal air temperatures. In another view, at least one climate model, which included coupled ice-ocean-atmosphere interactions [Manabe et al., 1992], gives the counter intuitive result that the sea ice cover would actually increase with global climate warming. The physical processes in the model that cause the predicted sea ice increase are: increased precipitation with a warmer atmosphere in polar regions, more snowfall on sea ice, lower-salinity in the near-surface ocean layers, more stable mixed-layer and reduced heat flux to the surface, and consequently more sea ice.

Clearly, if changes in the distribution of Antarctic sea ice are expected to be indicative of global climate change, a better understanding of the nature and causes of Antarctic sea ice variability is required. In particular, we should know whether Antarctic sea ice is expected to increase or decrease with climate warming. In this paper, we describe the variability of the Antarctic ice cover in detail, including the variations in regional sectors as defined in Zwally et al. [1983b] and Gloersen et al. [1992], using 20 years of well-calibrated data. We believe the characteristics of the observed sea ice variability of the Antarctic provide new insights to the interplay of the

relevant physical and climatic processes on seasonal to decadal time scales. In particular, our analysis of the decadal scale trends in sea ice by season show that the trend of increasing Antarctic sea ice cover is dominated by summer and autumn increases and that changes in the winter are near zero overall. These results are important, because the dominant climatic processes controlling the distribution of sea ice around the time of the winter maximum extent are likely to be significantly different than those near the summer minimum. Examination of potential correlations between temperature (using new satellite estimates of surface temperature averaged over the sea ice pack) and sea ice extent shows a wintertime correlation on a regional basis, which gives an estimate of the sensitivity of sea ice cover to temperature change.

2. Background

Since the advent of satellite remote sensing, the study of interannual changes in the Antarctic sea ice cover and their possible climatic significance have been the subject of numerous investigations. Initially, the use of relatively short or poorly calibrated satellite historical records caused some conflicting results regarding trends in ice extent [e.g., Kukla, 1978; Kukla and Gavin, 1981; Zwally et al., 1983a]. But even with the sole use of longer and more consistent passive microwave data, the trends from analysis of the same set of satellite data have differed [Johannessen et al., 1995; Bjorgo et al., 1997; Cavalieri et al., 1997; Stammerjohn and Smith, 1997]. This is partly because the satellite sensors have finite lifetimes and the time series is made up of measurements from different sensors, some of which have different footprints and characteristics than the others. Furthermore, different investigators use different ice algorithms for the retrieval of ice parameters, and their own techniques for removing abnormal values in the land/ocean boundaries and the open ocean. During periods of overlap, the different sensors also provide slightly different sea ice extents and actual areas, even with the same techniques. Therefore, further inter-sensor adjustments are required to match the overlap results and obtain a uniform time series.

For the period of November 1978 through December 1996, Cavalieri et al. [1997] found an

asymmetry in the trends of decreasing Arctic sea ice extent (- 2.9 ± 0.4%/decade) and increasing Antarctic sea ice extent (+ 1.3 ± 0.2%/decade). Cavalieri et al. [1997] also reviewed the results of previous analyses, which used essentially the same multi-satellite passive microwave data set, but with some different methodologies and conclusions about the apparent trends in the Antarctic sea ice. The methodologies for sea ice mapping and inter-satellite calibration techniques employed by Cavalieri et al. [1997] to produce a consistent multi-year data set are described in detail in Cavalieri et al. [1999]. Using these intercalibration methodologies Parkinson et al. [1999] further described the observed seasonal, regional, and interannual variability of the Arctic sea ice cover, finding an overall decreasing trend of - 34,300 ± 3700 km^2 /yr (-2.8%/decade), with significant decreases in all seasons (largest in spring and smallest in autumn).

3. Data and Techniques

The data for this paper are from the Scanning Multichannel Microwave Radiometer (SMMR) on the Nimbus 7 satellite (October 26, 1978 to August 20, 1987) and the Special Sensor Microwave/Imager (SSM/I) on several subsequent Defense Meteorological Satellite Program satellites. The SSM/I data set is actually from similar sensors on board three satellites: the F8 satellite (July 9, 1987 through December 18, 1991), the F11 satellite (December 3, 1991 through September 30, 1995), and the F13 satellite (May 3, 1995 through 1998). The SMMR usually provided data every other day and the SSMI's usually provided daily data for the indicated periods. Although the data period is described herein as 20-years, the actual period used in the analysis is the 20 years of 1979 though 1998 plus the two preceding months of November and December 1978. The exception is the analysis of the yearly and seasonal averages, which use only the full years 1979 through 1998.

Several algorithms have been developed for retrieving sea ice concentrations from multichannel passive microwave satellite data [e.g., see review by Steffen et al., 1992]. Long-term sea ice

climatologies from satellite microwave data using the NASA Team algorithm [Cavalieri et al., 1984; 1991; 1995; Gloersen and Cavalieri, 1986] and the Bootstrap algorithm [Comiso, 1986; Comiso, 1995] are currently archived at the National Snow and Ice Data Center (NSIDC), University of Colorado. A comparison of the performance of these two algorithms, during an entire annual cycle and for both hemispheres using SSM/I data in 1992, showed some significant differences in the calculated concentrations especially in the Weddell and Ross Seas of the Southern Ocean [Comiso et al., 1997]. The comparison also showed that the ice extents over a seasonal cycle as derived from both algorithms were very similar, but the Bootstrap algorithm gave some higher ice areas in the Southern Ocean than the Team algorithm.

The analysis and results in this paper use the second of two data sets archived at NSIDC, which is based on a modified NASA Team algorithm, consistent with recent publications [Parkinson et al., 1999; Gloersen et al., 1999]. The modified algorithm and other techniques used to create a unified time series for the second data set are described in Cavalieri et al. [1999], including elimination of bad data, interpolation of missing data, correction for instrumental drifts of the brightness temperature measurements, and reduction of false indications of sea ice from weather effects.

Additional procedures applied to the data analysis and described in Cavalieri et al. [1999] include accounting for land-to-ocean sensor spillover near coastal boundaries and intercalibration and algorithm adjustments using periods of data overlap. Of these, the intercalibration and algorithm adjustments, which used the overlap data to achieve a matching of both the derived sea ice extents and sea ice areas in the Antarctic to within 0.6%, were essential to producing a uniform time series with the required accuracy for climate change studies. This matching adjusted for effects of small sensor differences in the field-of-view and wavelength, and could not have been accomplished without the overlap of successive satellites.

A 6-week gap from December 3, 1987 through January 12, 1988 was filled in by non-linear interpolation as described in Gloersen et al. [1999]. Briefly, multiple ordinary least squares

(MOLS) regression is used for this purpose. This procedure invokes 12 linear components to produce a model fit of the gridded data at each grid point. These are described by the equation

$$y = a_0 + a_1 t + \sum_{k=1}^{5} [a_{2k} \cos(2\pi kt / \tau) + a_{(2k+1)} \sin(2\pi kt / \tau)] \tag{3.1}$$

where τ is the annual cycle period (365.25 days), t is the time, and y is the model fit to the data. The data gap was filled with values generated by the MOLS, using coefficients derived from that part of the F8 SSMI data set consisting of 60 days before and 60 days after the gap.

Calculated ice concentrations are mapped to a 25 x 25 km grid on a polar stereographic projection [NSIDC, 1992] in daily maps (every other day for most of the SMMR time period). Figure 1 shows average sea ice concentration maps for the times of the seasonal minimum coverage in February and the maximum coverage in September, respectively for the first and last 10 years and their differences. Monthly-average maps are created by averaging daily maps, and multi-year averages by averaging the monthly maps.

Sea ice extent is defined as the cumulative area of all grid cells having at least 15% sea ice concentration. Sea ice area is defined as the cumulative area of the ocean actually covered by sea ice, and is calculated by summing the product of the area of grid cells and their sea ice concentration. The ice-free area within the ice pack is the area of ice-free ocean within the pack, calculated as the difference: ice extent - ice area. Parkinson et al. [1999] showed, using Arctic data, that essentially the same trends are deduced using different cutoffs of 15, 20, and 30% for the definition of ice extent, which implies that the trends are not sensitive to the exact definition of ice extent.

Analysis of trends using alternative algorithms requires careful application of similar techniques for creating a unified time series. A recent analysis of trends using the Bootstrap algorithm by

one of us [JC] produces increases in Antarctic sea ice area similar to the Team algorithm, but produces a small negative trend for ice extent (even though the Bootstrap and Team algorithms agree better in their determinations of extent than area). However, the trends from the two algorithms do agree in both extent and area for the separate periods of SMMR and SSMI data, which implies a different inter-sensor matching by the Bootstrap algorithm. A significant difference between the long-term trends in ice extent and ice area would imply a long-term trend in ice concentration and the state of convergence/divergence and perhaps thickness of the ice pack. While such changes in ice concentration do occur seasonally and interannually, a trend in ice concentration over 20 years is likely to be smaller than would be implied by the difference in extent and area trends indicated by the Bootstrap algorithm. The smaller difference between the long-term trends in extent and area with the Team algorithm is discussed in Section 4. In the Arctic, long-term trends in both ice extent and area from the two algorithms are in close agreement. Also, a recent analysis of Antarctic sea ice trends for 1978 to 1996 by Watkins and Simmonds [2000] found significant increases in both Antarctic sea ice extent and ice area, similar to the results in this paper.

Several methods are used in this paper to calculate linear trends, all of which attempt to remove the seasonal cycle and other periodic variations from the trend calculation. One method is to calculate deviations of parameters from averages of the parameters, and then use ordinary least squares (OLS) fits to the deviations (or monthly anomalies) shown in Figures 2b to 19b. This method provides the yearly trends over the 20-year period as given in Tables 4, 6, and 8. A second method applies OLS to yearly and seasonal averages, as shown in Figures 2c-19c and Tables 5, 7, and 9. The third method, multiple ordinary least squares (MOLS), takes into account the 3- to 5-year periodicity in the monthly deviations. We fit a multivariate linear and sinusoidal function with a period of 3, 4, or 5 years to the monthly deviations (Figures 2b to 19b). The four fitted parameters are the amplitude, phase, intercept, and linear slope (Tables 4, 6, and 8).

Maps of trends are made using two methods. Band-Limited Regression (BLR) is applied to each

of the grid points in the 20-year time series of sea ice concentration maps giving the overall trend maps in Figure 20, extending the previous 18.2-year trend maps [Gloersen, et al., 1999]. The BLR technique has been described in detail elsewhere [Lindberg, 1986; Lindberg and Park, 1987; Kuo et al., 1990]. Briefly, the technique involves the application of a narrow-bandpass filter comprised of multiple prolate spheroid windows, while determining the trend of the data series and its standard deviation. The narrow bandpass filter serves to eliminate oscillations with periods less than about 1/4 of the time interval of the observations, in this case periods less than 5 years. The trends and standard deviations are obtained as described by Draper and Smith [1981], but with the substitution of the truncated sinc matrix obtained by reconstruction from the first eight of the singular value decomposition components of the full sinc matrix [Gloersen and Campbell, 1991] for the traditional variance matrix. For the seasonal trend maps (Figure 21), we use MOLS (Eq. 3.1) with 10 oscillatory terms, because the BLR technique does not lend itself to time series with large temporal gaps. MOLS removes a model seasonal cycle simultaneously with the determination of the trend line.

4. Characteristics of Antarctic Sea Ice Regions

Unlike the northern hemisphere sea ice cover, the sea ice cover in the southern hemisphere surrounds the continent with no outer land boundaries and peripheral seas. The ice cover is affected by many environmental factors such as surface air temperature, wind, ocean current, tides, and sea surface temperature. The predominant factor affecting the sea ice is the seasonal cycle of solar insolation and temperature that drives the freezing and melting of ice within each sector. A major factor causing interannual variations of the ice extent is shifts in the large scale atmospheric circulation and in particular the position of the Antarctic circumpolar trough [e.g., Cavalieri and Parkinson, 1981; Carleton, 1989, and Enomoto et al., 1992]. A key feature of the Southern Ocean is the Antarctic Circumpolar Current (ACC) [Deacon, 1937]. Driven by prevailing westerly winds north of about 65° S, the ACC provides the major exchange of water between the Atlantic and Pacific Oceans. The ACC also plays an important role in the

thermohaline circulation which influences climate by redistributing heat, freshwater and other properties around the globe. Because of the massive eastward flow of the ACC, the outer part of the sea ice cover also moves around the continent transporting some ice between sectors. Also, a coupled ocean-atmosphere phenomenon, called the Antarctic Circumpolar Wave (ACW), appears to make a complete cycle around the continent every 8-9 years [White and Peterson, 1996], affecting the ice regionally with a periodicity of about 4 years. Within about 5° of the Antarctic coast, the flow is mainly westward driven by the East Wind Drift, and the region of the Antarctic divergence lies between the eastward and westward flows. The five regional sectors [Zwally et al., 1983b] dividing the ice pack for our analysis of sea ice variability and trends are given in Table 1.

Table 1. Regional Sectors of the Southern Ocean

SECTOR	LONGITUDE RANGE
Weddell Sea	60° W to 20° E
Indian Ocean	20° E to 90° E
Western Pacific Ocean	90° E to 160° E
Ross Sea	160° E to 130° W
Bellingshausen-Amundsen Seas	130° W to 60° W

The Weddell Sea is regarded as one of the primary sources of global bottom water [Deacon, 1937; Foster and Middleton, 1979; Zwally et al., 1985]. The presence of the large ocean shelf region adjacent to the Antarctic Peninsula and the Ronne and Filchner ice shelves (30° - 80° W) influences formation of Antarctic Bottom Water [Fahrbach et al., 1995; Gordon et al., 1993]. As ice forms in the coastal polynyas and areas of ice divergence along the shelf, the rejected brine is mixed with shelf water which in turn becomes saline and cold, eventually having the characteristics of bottom water. A large fraction of the ice cover in the Weddell Sea is also postulated to originate from ice formed at the coastal polynyas [Zwally et al., 1985; Lange et al.,

1989; Comiso and Gordon, 1998]. Also, Comiso and Gordon [1998] show coherence in the interannual variations in the polynya areas with the Antarctic Circumpolar Wave, suggesting the influence of the latter not just in the interannual change in the ice cover but also in bottom water formation.

The Weddell Sea is also the site of a large deep-ocean polynya observed only in 1974, 1975, and 1976, named the Weddell polynya [Zwally and Gloersen, 1977; Carsey, 1980; Parkinson, 1983; Martinson et. al., 1981; Gordon and Comiso, 1988]. The temperature of the water column to 2,500 m depth decreased by about 0.8°C from pre-polynya to post-polynya years, suggesting deep convection in the region during the occurrence of the polynya [Gordon and Comiso, 1988].

The Indian Ocean sector is the site of many mesoscale phenomena. Wakatsuchi et al. [1994] reported the existence of many open ocean low concentration features in the ice pack associated with the formation of eddies. A persistent feature in the region adjacent to Cape Ann (52° E) is the Cosmonaut Polynya, which has been studied by Comiso and Gordon [1996] and postulated to be initiated by cyclones but sustained by current-current interaction that causes the upwelling of warm water and melts the ice. The polynya has also been studied by Takizawa et al. [1994] and they also point out that the polynya is likely a sensible heat polynya initiated by atmospheric convergence near the region of the Antarctic Divergence in the ocean.

The Western Pacific Ocean Sector is the sector with the average continental boundary that is farthest from the South Pole. Not surprisingly it has the least ice cover among the 5 sectors. Surface measurements also indicate that the ice cover may be the thinnest (averaging about 45 cm) among the sectors [Worby et al., 1998]. This is probably because the ice season is shortest in this sector and drifting buoy observations have indicated that the ice cover is generally divergent and therefore dominated by leads and thin ice [Allison, 1989]. It has also been reported that polynyas have been active along the Wilkes Land coast (100° - 150° W) [Cavalieri and Martin, 1985] and are regarded as among the significant sources (in addition to the Weddell and Ross Seas) of Antarctic Bottom Water [Rintoul, 1998].

The Ross Sea sector has the second largest ice extent among the five sectors during winter. This is not surprising since the region is one of the coldest and the land/ocean boundary in this sector is on the average closest to the South Pole. However, persistent synoptic winds off the Ross Ice Shelf (150° W - 160° E) and katabatic surge events cause the formation of a large coastal polynya during spring and reduced ice concentrations in winter (Zwally et al, 1985 and Bromwich et al, 1998]. The front of the Ross Ice Shelf is free of sea ice during the summer, and sea ice in western part of the Ross Sea is generally advected northward into warmer water.

The Bellingshausen/Amundsen (B/A) Seas sector is the only sector other than the Weddell Sea with substantial multiyear ice. The region has been noted for its thick and impenetrable ice pack that has caused ships to be beset for several months during winter. However, the extent of multiyear ice decreased substantially during the summers of 1989 to 1994, as reported by Jacobs and Comiso [1997] and Stammerjohn and Smith [1997], the latter identifying the effect as part of an opposing climate pattern. The ice extent in the region was found by Jacobs and Comiso [1993] to be strongly correlated to surface temperature, which has been shown to be on the rise in the Antarctic Peninsula [e.g., King, 1994; Stammerjohn and Smith, 1997].

5. Variability and Trends in Sea Ice Extent, Area of Sea Ice, and Open Water Within the Extent Boundary.

The maps of the change in sea ice concentrations between the first and second halves of the 20-year period shown in Figure 1 illustrate the spatial distribution of the principal changes in the sea ice cover. In winter, decadal changes in the inner part of the ice pack are small. In contrast, near the ice edge significant changes of more than 10% ice concentration occurred for several hundred kilometers north-south distance However, decreases in the Weddell Sea and the Western Pacific Ocean sectors are approximately offset by increases in the Ross Sea, Amundsen Sea, and Indian Ocean. In summer, concentration changes are evident throughout the ice pack, with the largest

decreases in the Bellingshausen-Amundsen Seas sector. In the Weddell Sea, decreases occurred along the coast of the Antarctic Peninsula with significant increases to the east due to a more eastward extension of the pack in the later years. As shown in the following analysis, the overall trend in both sea ice extent and sea ice area is positive over the 20 years, with the largest sea ice increases occurring in the fall and summer seasons.

The Antarctic sea ice cover varies substantially during a seasonal cycle and significantly from one year to another, as indicated by the time series of monthly ice extents, sea ice areas, and open water areas within the pack from November 1978 through December 1998 shown in Figure 2a to 19a. The 20-year average of the seasonality of the ice cover, shown in the inset of Figure 2, shows an ice cover that typically varies from 3.5 x 10^6 km^2 in summer to 17.4 x 10^6 km^2 in winter (see inset in Figure 2). This is consistent with previously published values [Zwally et al., 1983b; Gloersen et al., 1992; Cavalieri et al., 1997]. During the 20-year period, the maxima and minima vary substantially. The highest extent occurs in the winter of 1998 at 18.8 x 10^6 km^2, and the lowest value occurs in the summer of 1993 at 2.46 x 10^6 km^2 based on the monthly-averaged values. The association of periods of above average ice extents in winter with and below average extents in the preceding or following summer indicate a modulated distribution, as noted previously [Zwally et al., 1985; Comiso and Gordon, 1998]. The period of the modulation is about 4 years, consistent with the periodicity of the passing of the Antarctic Circumpolar Wave (ACW) at a given region [White and Peterson, 1996].

For Figures 2b to 19b, the seasonal cycle is removed from the sea ice extent, sea ice area, and open water within the pack by calculating the monthly deviations from the 20-year averages (20 years plus 2 months) for each month. For Figures 2c to 19c, the seasonal cycle is removed in the yearly averages of the monthly values, and seasonal values are calculated as averages for four seasons (Summer: January, February, and March; Fall: April, May, and June; Winter: July, August, and September; and Spring: October, November, and December).

The variability of the extent of the ice pack on monthly to decadal time scales is calculated

as the standard deviations (σ_y) of the points about the linear fits to the monthly deviations (Table 2). Similarly, the interannual variability for the yearly averages and the four seasons is calculated as the standard deviations of the points about the linear fits to the yearly and seasonal averages. Although these values include a measurement error, the primary variation is in the ice cover. In general, the variability decreases with larger spatial and longer temporal averaging as expected. For example, the overall monthly variability is comparable in magnitude (3.85×10^5 km^2) to the monthly variability in the individual sectors (1.77 to 3.37×10^5 km^2), but is smaller (3.4%) as a percentage of the mean extent than the sector values (8.0 to 14.7%). This is due to the spatial averaging over positive and negative anomalies that tend to offset each other among the sectors. Also, the variability in the monthly values for the total Southern Ocean (4.50×10^5 km^2) is larger than the interannual variability in the yearly values (1.78×10^5 km^2) due to temporal averaging. The variabilities in Table 2 can be interpreted as the deviation from the monthly mean that will be exceeded approximately 32% of the time. Likewise, the variabilities in Table 3 can be interpreted as the deviation from the yearly or seasonal means that will be similarly exceeded.

In Figure 2b, the variability, σ_y, for the total ice pack appears to be larger for the first 10 years than it is for the last 10 years (respectively 4.50 and 3.11×10^5 km^2). The largest decreases are in the W. Pacific and Ross Sea sectors, with small decreases in the Weddell Sea and Bellingshausen-Amundsen Seas and an increase in the Indian Ocean Sector. Primary causes of ice variations are shifts in the atmospheric temperature distribution that affect the ice growth and decay and shifts in the atmospheric circulation that affect the forcing of the north-south position of the ice edge. However, during a season significant areas of ice cover can move from one sector to another, so the results from each sector are not strictly associated with ice that grows and decays locally. Therefore, some of the sector to sector variability may be correlated due to ice advection, as well as by atmospheric and oceanographic connections. If the variations among sectors are not correlated, then the square-Root of the Sum of the Squares (RSS) of the sector values (Table 2) should equal the variability for the total Southern Ocean. However, for the first 10 years, the RSS is less than the total variability (4.04 vs 4.50) and in the second 10 years it is greater (3.62 vs 3.11). Therefore, not only did the variability decrease in most regions,

but the during the first period the sector anomalies were less effective in offsetting each other in the overall spatial average, further reducing the overall variability between the two periods.

On the basis of yearly means, the interannual variability in ice extent is only 1.6% for the total pack and ranges from 5.6% to 8.1% by sector. By season, the variabilities are on average about 2 times as large as the yearly value, as is statistically expected from averaging. Seasonally, the variability is generally smallest in the winter and largest in the summer, particularly as a percentage of the mean extents. Regionally, the variabilities are smallest in magnitude in the Indian and W. Pacific sectors, but on a percentage basis there is little sector to sector difference in the variabilities.

Analysis of long trends in the sea ice cover not only requires removal of the average seasonal cycle, but should also account for periodic interannual variability that can affect the calculated linear trend. For Figures 2b to 19b, the seasonal cycle is removed by calculating the monthly deviations from the 20-year average for each month. The OLS fits to these deviations are the yearly trends listed in Tables 4, 6, and 8. A less-effective method of removing the seasonal cycle applies OLS fits to yearly averages of the sea ice parameters, giving the yearly trends in Tables 5, 7, and 9. This method also gives the trends by season listed in Tables 5, 7, and 9. Since the yearly averages do not include November and December 1978, the OLS trends for ice extent excluding these two months are also listed in parenthesis in Table 4 for comparison. The third method (MOLS) takes into account the 3 to 5 year periodicity in the monthly deviations, as well as the seasonal cycle, by fitting a multivariate linear and sinusoidal function with a period of 3, 4, or 5 years. The respective slopes and amplitudes for ice extent, ice area, and open water are given in Tables 4, 6, and 8 for the period (3, 4, or 5 years) that had the largest amplitude of the sinusoidal fit to ice extent. The corresponding linear and interannual cycles are plotted over the monthly deviations in Figures 2b to 19b. In cases where, for example, 3 and 4 year fits have nearly the same amplitudes, a somewhat better fit might be obtained for a fractional year cycle. Or if the frequency of the interannual variability changes during the 20-years (non-stationary cycle), a variable period might be more appropriate. Our selection of the best fit for integer-year

periodicity in the range of 3 to 5 years is intended to quantify a primary periodic component of the interannual variability in a simple representation.

The phases, given in Table 4 as the time of the first peak, are all for the 4 year period with the parenthesis indicating values for sectors that have the largest amplitude for a period other than the one selected by ice extent amplitude. Some progression in phase is indicated from the Weddell Sea, to the Indian Ocean, and to the W. Pacific, but not consistently around the continent. In Tables 6 and 8, where the amplitude of the ice area or open water was somewhat larger for a another period than the one for ice extent, that period is indicated in parenthesis.

The derived 20-yr trend in sea ice extent from the monthly deviations of $13.44 \pm 4.18 \times 10^3$ km^2/year or $1.18 \pm 0.37\%$ per decade for the entire Antarctic sea ice cover is significantly positive. The trend in the integrated area of sea ice within the extent boundary is somewhat larger: $16.96 \pm 3.84 \times 10^3$ km^2/year or $1.96 \pm 0.44\%$ per decade. The multivariate MOLS values are selected as the preferred values, because of the reduced sensitivity of the fits to periodic interannual variations. Nevertheless, the linear trends for three methods agree well and conclusions about the long-term trends are not affected by the choice of methods. The differences between the MOLS and the OLS of the monthly deviations using the 20-year calculation, are 0.09σ overall and 0.55σ, 0.79σ, 0.61σ, 0.29σ, and 0.36σ in the respective sectors. The 20-year values are in slightly better agreement in most cases than the 20.17 year values, because the deviations for the two months of 1978 are positive and the MOLS periodic function is also positive at that time. The differences between the MOLS and the OLS of the yearly averages, are 0.05σ overall and 0.54σ, 0.79σ, 0.62σ, 0.25σ, and 0.37σ in the respective sectors.

A measure of the fraction of the monthly to interannual variability represented by the interannual sinusoidal cycle is defined as the ratio of the RMS of the sine wave (i.e. p-p amplitude x 0.707/2) to the residual variability about the linear trend in the monthly deviations (i.e. the σ_y in Table 2). In the Indian Ocean and the Bellingshausen-Amundsen Seas sectors, the respective fractions of

Table 2. Monthly to Interannual Variability (σ_y) in Sea Ice Extent from Monthly Deviations

Sector	First 10 Years		Second 10 Years		Over 20 Years	
	10^5 km^2	% of mean	10^5 km^2	% of mean	10^5 km^2	% of mean
Southern Ocean	4.50	3.9	3.11	2.7	3.85	3.4
Weddell Sea	3.45	8.2	3.31	7.9	3.37	8.0
Indian Ocean	1.58	8.6	1.96	10.6	1.77	9.6
W. Pacific Ocean	1.66	14.0	1.40	11.9	1.53	12.9
Ross Sea	3.25	12.0	2.28	8.4	2.80	10.3
Bellingshausen/ Amundsen Seas	2.22	15.4	2.06	14.2	2.14	14.7
RSS of sectors	4.04		3.62		3.82	

Table 3. Interannual Variability (σ_y) in Sea Ice Extent from Yearly and Seasonal Averages

Sector	Yearly		Summer (JFM)		Fall (AMJ)		Winter (JAS)		Spring (OND)	
	10^5 km^2	% of mean	10^5 km^2	% of mean	10^5 km^2	% of mean	10^5 km^2	% of mean	10^5 km^2	% of mean
Southern Ocean	1.78	1.6	3.16	8.0	4.49	4.5	2.20	1.3	3.62	2.5
Weddell Sea	2.37	5.6	2.43	16.6	2.65	7.4	3.77	6.0	3.55	6.6
Indian Ocean	1.17	6.3	0.67	22.3	1.66	12.9	1.57	5.1	2.07	7.8
W. Pacific Ocean	0.96	8.1	0.98	21.2	0.92	8.5	1.66	9.3	1.59	11.5
Ross Sea	1.95	7.2	2.44	24.6	3.04	11.3	2.43	6.3	2.39	7.1
Bellingshausen/ Amundsen Seas	1.35	9.3	1.12	16.0	1.77	13.9	2.36	11.3	2.25	13.1

Table 4. 20.2-year Trends in Sea Ice Extent (area with C> 15%) 1979- 1998 from Monthly Deviations

Sector	Yearly Trend (OLS) 20.17 yrs (20 yrs)		Mean Extent	Multivariate Yearly Trend and 3 to 5 Year Cycle					
	10^3 km^2/yr	%/dec	10^6 km^2	10^3 km^2/yr	%/dec	Period Years	P-P Amplitude 10^5 km^2	% of variability (see text)	Phase (1st peak) for 4 yr period
Southern Ocean	12.42 ± 4.24 (13.05 ± 3.85)	1.09 ± 0.37 (1.17 ± 0.38)	11.410	**13.44 ± 4.18**	**1.18 ±0.37**	3	2.17 ± 0.49	20	(Jul 82)
Weddell Sea	4.40 ± 3.71 (4.48 ± 3.37)	1.05 ± 0.88 (1.07 ± 0.89)	4.206	**6.46 ± 3.62**	**1.54 ± 0.86**	4	2.64 ± 0.42	28	Mar 80
Indian Ocean	0.36 ± 1.96 (-0.08 ± 1.98)	0.20 ± 1.06 (-0.04 ± 1.07)	1.845	**-1.50 ± 1.81**	**-0.81 ± 0.98**	4	2.09 ± 0.21	42	Sep 81
Pacific Ocean	3.27 ± 1.69 (3.67 ± 1.71)	2.77 ± 1.43 (3.11 ± 1.45)	1.181	**2.65 ± 1.68**	**2.44 ± 1.42**	5	1.02 ± 0.19	24	(Nov 82)
Ross Sea	18.12 ± 3.07 (17.92 ± 3.13)	6.64 ± 1.13 (6.57 ± 1.15)	2.729	**18.78 ± 3.01**	**6.91 ± 1.11**	3	1.89 ± 0.35	24	(Feb 82)
Bellingshausen/ Amundsen Seas	-13.74 ± 2.36 (-12.95 ± 2.38)	-9.48 ± 1.63 (-8.94 ± 1.65)	1.449	**-13.75 ± 2.22**	**9.49 ±1.53**	4	2.31 ± 0.26	38	Nov 82

Table 5. 20-year Trends in Sea Ice Extent (area with C> 15%) 1979- 1998 from Yearly and Seasonal Averages

Sector	Yearly		Summer (JFM)		Fall (AMJ)		Winter (JAS)		Spring (OND)	
	10^3 km^2/yr	%/dec	10^3 km^2/yr	%/dec	10^3 km^2/yr	%/dec	10^3 km^2/yr	%/dec	10^3 km^2/yr	%/dec
Southern Ocean	13.24 ± 6.91	1.16 ± 0.61	8.8 ± 12.2	2.2 ± 3.1	26.4 ± 17.4	2.7 ± 1.8	7.4 ± 8.5	0.4 ± 0.5	10.1 ± 14.0	0.7 ± 1.0
Weddell Sea	4.50 ± 9.20	1.07 ± 2.19	11.3 ± 9.4	7.7 ± 6.4	12.2 ± 10.3	3.4 ± 2.9	-0.5 ± 14.6	-0.1 ± 2.3	-4.9 ± 13.8	-0.9 ± 2.5
Indian Ocean	-0.07 ± 4.52	-0.04 ±2.45	1.8 ± 2.6	6.0 ± 8.7	4.5 ± 6.4	3.5 ± 5.0	- 6.1 ± 6.1	-2.0 ± 2.0	-0.4 ± 8.0	-0.2 ± 3.0
Pacific Ocean	3.69 ± 3.70	3.13 ± 3.14	6.7 ± 3.8	14.5 ± 8.2	8.5 ± 3.6	7.8 ± 3.3	2.3 ± 6.4	1.3 ± 3.6	–2.6 ± 6.2	-1.9 ± 4.5
Ross Sea	18.04 ±7.56	6.61 ± 2.77	12.1 ± 9.5	12.2 ± 9.5	14.0 ± 11.8	5.2 ± 4.4	14.2 ± 9.4	3.7 ± 2.5	31.6 ± 9.3	9.4 ± 2.8
Bellingshausen/ Amundsen Seas	-12.92 ±5.25	-8.92 ± 3.62	-23.1 ± 4.3	-32.9 ± 6.2	-12.8 ± 6.9	-10.1 ±5.4	-2.4 ± 9.1	-1.2 ± 4.4	-13.5 ± 8.7	-7.9 ± 5.1

Table 6. 20.2-year Trends in Area of Sea Ice Within the Extent Boundary (C> 15%) 1979- 1998 from Monthly Deviations

Sector	Yearly Trend (OLS) 20.17 yrs		Mean Area	Mean C	Multivariate Yearly Trend and 3 to 5 Year Cycle				
	10^3 km^2/yr	%/dec	10^6 km^2	%	10^3 km^2/yr	%/dec	Period Years	P-P Amplitude 10^5 km^2	% of variability (see text)
Southern Ocean	15.82 ± 3.94	1.83 ± 0.45	8.644	76	**16.96 ± 3.84**	**1.96 ± 0.44**	3	2.57 ± 0.45	25
Weddell Sea	3.38 ± 3.16	1.01 ± 0.94	3.359	80	**4.81 ± 3.14**	**1.43 ± 0.94**	4 (3)	1.70 ± 0.36	21
Indian Ocean	0.51 ± 1.67	0.38 ± 1.24	1.352	73	**-1.22 ± 1.52**	**-0.90 ± 1.13**	4	1.93 ± 0.18	45
Pacific Ocean	5.33 ± 1.31	6.61 ± 1.62	0.805	68	**4.92 ± 1.30**	**6.11 ± 1.62**	5 (3)	0.74 ± 0.15	22
Ross Sea	15.82 ± 2.58	7.54 ± 1.23	2.097	77	**16.39 ± 2.53**	**7.82 ± 1.21**	3	1.46 ± 0.29	22
Bellingshausen/ Amundsen Seas	-9.21 ± 1.82	-8.95 ± 1.77	1.029	71	**-9.52 ± 1.72**	**-9.25 ± 1.67**	4	1.76 ± 0.20	38

Table 7. 20-year Trends in Area of Sea Ice Within the Extent Boundary (C> 15%) 1979- 1998 from Yearly and Seasonal Averages

Sector	Yearly		Summer (JFM)		Fall (AMJ)		Winter (JAS)		Spring (OND)	
	10^3 km^2/yr	%/dec	10^3 km^2/yr	%/dec	10^3 km^2/yr	%/dec	10^3 km^2/yr	%/dec	10^3 km^2/yr	%/dec
Southern Ocean	16.7 ± 6.7	1.9 ± 0.8	7.4 ± 9.1	2.9 ± 3.5	36.1 ± 16.0	4.8 ± 2.1	13.4 ± 8.7	1.0 ± 0.6	9.8 ± 13.8	0.9 ± 1.3
Weddell Sea	3.5 ± 7.3	1.0 ± 2.2	8.6 ± 8.4	8.1 ± 7.9	13.3 ± 8.8	4.5 ± 3.0	-2.1 ± 11.6	-0.4 ± 2.2	-5.7 ± 11.3	-1.4 ± 2.7
Indian Ocean	0.3 ± 4.0	0.2 ± 3.0	0.9 ± 1.9	5.3 ± 10.9	5.4 ± 5.5	5.8 ± 6.0	-2.5 ± 5.8	-1.0 ± 2.4	-2.6 ± 7.0	-1.4 ± 3.8
Pacific Ocean	5.6 ± 2.7	7.0 ± 3.4	6.5 ± 2.8	22.7 ± 9.7	9.5 ± 2.9	12.7 ± 3.9	4.6 ± 5.4	3.7 ± 4.3	2.0 ± 4.2	2.2 ± 4.6
Ross Sea	15.8 ± 6.1	7.5 ± 2.9	8.4 ± 6.2	14.4 ± 10.6	15.3 ± 10.3	7.2 ± 4.9	12.4 ± 8.3	4.0 ± 2.7	26.9 ± 7.8	10.6 ± 3.1
Bellingshausen/ Amundsen Seas	-8.5 ± 4.1	-8.3 ± 3.9	-17.1 ± 3.7	-37.8 ± 8.1	-7.3 ± 5.2	-8.4 ± 5.9	1.0 ± 7.1	0.6 ± 4.6	-10.7 ± 6.2	-8.6 ± 4.9

Table 8. 20.2-year Trends in Open Water Area Within the Extent Boundary (C> 15%) 1979- 1998 from Monthly Deviations

Sector	Yearly Trend (OLS) 20.17 yrs		Mean Open Water	Multivariate Yearly Trend and 3 to 5 Year Cycle				
	10^3 km^2/yr	%/dec	10^6 km^2	10^3 km^2/yr	%/dec	Period Years	P-P Amplitude 10^5 km^2	% of variability (see text)
Southern Ocean	-3.41 ± 1.87	-1.23 ± 0.67	2.767	**-3.52 ± 1.87**	**-1.27 ± 0.67**	3 (4)	0.66 ± 0.22	14
Weddell Sea	1.02 ± 1.38	1.20 ± 1.63	0.847	**1.65 ± 1.34**	**1.95 ± 1.59**	4	0.98 ± 0.16	28
Indian Ocean	-0.15 ± 0.70	-0.30 ± 1.42	0.493	**-0.28 ± 0.71**	**-0.57 ± 1.44**	4 (5)	0.16 ± 0.08	9
Pacific Ocean	-2.06 ± 0.56	-5.47 ± 1.50	0.376	**-2.27 ± 0.57**	**-6.04 ± 1.51**	5 (3)	0.28 ± 0.07	19
Ross Sea	2.31 ± 0.99	3.65 ± 1.56	0.632	**2.39 ± 0.98**	**3.78 ± 1.55**	3	0.49 ± 0.11	19
Bellingshausen/ Amundsen Seas	-4.53 ± 0.82	-10.80 ± 1.96	0.420	**-4.23 ± 0.79**	**-10.07 ± 1.89**	4 (5)	0.66 ± 0.09	32

Table 9. 20-year Trends Open Water Area Within the Extent Boundary (C> 15%) 1979-1998 from Yearly and Seasonal Averages

Sector	YEARLY		Summer (JFM)		Fall (AMJ)		Winter (JAS)		Spring (OND)	
	10^3 km^2/yr	%/dec	10^3 km^2/yr	%/dec	10^3 km^2/yr	%/dec	10^3 km^2/yr	%/dec	10^3 km^2/yr	%/dec
Southern Ocean	-3.5 ± 3.2	-1.3 ± 1.1	1.4 ± 6.0	1.0 ± 4.4	-9.7 ± 2.9	-4.2 ± 1.2	-6.0 ± 3.7	-1.7 ± 1.0	0.3 ± 6.0	0.1 ± 1.6
Weddell Sea	1.0 ± 3.1	1.2 ± 3.7	2.6 ± 3.5	6.6 ± 8.8	-1.0 ± 2.3	-1.6 ± 3.5	1.6 ± 3.8	1.5 ± 3.6	0.8 ± 6.2	0.6 ± 4.9
Indian Ocean	-0.3 ± 0.8	-0.7 ± 1.7	0.9 ± 1.0	6.9 ± 8.0	-0.9 ± 1.1	-2.4 ± 3.1	-3.6 ± 1.7	-5.4 ± 2.6	2.2 ± 1.9	2.7 ± 2.4
Pacific Ocean	-1.9 ± 1.2	-5.2 ± 3.1	0.2 ± 1.2	1.3 ± 6.7	-1.0 ± 1.0	-3.0 ± 2.7	-2.4 ± 1.5	-4.6 ± 3.0	-4.6 ± 2.5	-9.8 ± 5.2
Ross Sea	2.2 ± 2.1	3.5 ± 3.4	3.7 ± 4.0	9.0 ± 9.7	-1.3 ± 2.6	-2.3 ± 4.6	1.8 ± 2.3	2.4 ± 3.1	4.7 ± 2.8	5.8 ± 3.4
Bellingshausen/ Amundsen Seas	-4.4 ± 1.6	-10.5 ± 3.8	-6.0 ± 1.7	-24.0 ± 6.8	-5.5 ± 2.1	-14.1 ± 5.3	-3.4 ± 2.6	-6.1 ± 4.6	-2.8 ± 3.3	-6.0 ± 7.0

the variability in the sine wave of 42% and 38% are largest, and the fitted interannual cycle appears to follow the variation of the monthly deviations better than in the other sectors (< 28%) and the total (20%) (see Table 4). If compared to the variability in the yearly averages (Table 3), the fractions are 1.4 to 2.2 times larger. The fractions of the variability of the sine wave in sea ice area are similar to those for ice extent, and the fractions for open water are somewhat smaller.

The larger rate of increase in the area of sea ice, compared to the rate of increase in sea ice extent in % of mean/decade, implies that the average concentration within the extent boundary is increasing and the ice pack is becoming more compact. The area of open water within the ice extent is also decreasing, as is also shown in the calculated trends in open water given in Table 9. However, the trend in open water is not by itself an indicator of a change in average concentration. If for example, the ice extent and the ice area were increasing by the same percentage rates, then the average ice concentration would remain unchanged, but the amount of open water would be increasing at the same rate as the extent and area (the area in which open water can occur is increasing). However, the observed trend in open water area is negative (-1.27 ± 0.67%/decade) compared to positive trends in ice extent (1.18 ± 0.37%/decade) and ice area (1.96 ± 0.44%/decade). The observed rates of change in extent and area imply that the average ice concentration is increasing 0.77% of concentration/decade (i.e. (1- 1.0196/1.0118) x100). The implied change in concentration is 0.59%/decade (0.77% of 76% mean concentration), which corresponds to trend in open water of -6.68×10^3 km^2/year (-2.42%/decade). These implied changes in open water have the same sign as the trends calculated directly from the open water deviations (monthly extent - monthly area), but are nearly twice as large. Seasonally, this effect appears to be largest in the fall and smallest in the spring. However, this phenomena is not consistent in all sectors, with the largest implied yearly average increase in concentration of 2.44%/decade in the W. Pacific Ocean, a smaller 0.66%/decade change in the Ross Sea, and small changes in Bellingshausen-Amundsen Seas (0.19%/decade), Indian Ocean (-0.07%/decade) and the Weddell Sea (-0.09%/decade). In contrast, Watkins and Simmonds [2000] found an increasing trend in open water (and deceasing concentration), as well as increasing trends in ice extent and ice area, but their data might not have been intercalibrated

to match ice extents and sea ice areas during the overlap periods.

Despite the residual uncertainties in deriving ice concentrations, we believe time series of open water in Figures 15-19 illustrate characteristics of the interannual variability and seasonality of the variability that are interesting and likely to be real sea ice variations. The figures are also useful for assessing the reality of these variations in relation to possible instrumental effects, errors, or variations is sea ice properties such as flooded snow cover. For examples of these variations are: 1) the small seasonal amplitude in the Ross Sea in 1986 and an increasing trend in open water through about 1988 followed by a decrease, 2) the constancy of the seasonal amplitude for the total ice pack, in contrast to the large variability in seasonal amplitude in Weddell, Ross, and BA sectors, and 3) the consistent decreasing trend in the BA sector. These are characteristics that are unlikely to be algorithm or instrument dependent. Furthermore, the data presented in this figures should be useful to further investigations, for example, can the variation in amplitude in the Ross Sea in 1986 be explained by variations in wind-induced divergence?

If in fact the sea ice pack is becoming more compact in some regions, a probable cause would be reduction in the forcing of the ice divergence by the wind fields. As noted in the above discussion of variability, the W. Pacific Ocean and the Ross Sea sectors also had a decrease in variability from the first half of the analysis period to the second, which would be consistent with an increase in concentration and lesser divergent forcing of the ice pack. The potential climatic significance of such a trend in ice concentration and open water justifies further studies, such as determining whether there is a corresponding change in the wind fields.

Interannually, the variations in ice extent, ice area, and open water are almost exactly in phase in each of the five sectors, as shown by the 3 to 4 year sinusoidal functions in the multivariate fits. For the total ice pack, the cyclical variation in open water is out of phase with the ice extent and the ice area by about 1 year, which is probably not significant since the sector-by sector variations in the three parameters are very much in phase.

Trends for each of the four seasons are obtained from OLS fits to 3-month averages for summer (January, February, and March), Fall (April, May, and June), Winter (July, August, and September), and Spring (October, November, and December). The overall trends in sea ice extent and sea ice area are also positive in all seasons (Figures 2c and 8c and Tables 5 and 7), the most positive being in the fall season ($26.4 \pm 17.4 \times 10^3$ km^2/year and 2.7 ± 1.8%/decade in ice extent). However, the small positive trends in winter ice extent ($7.4 \pm 8.5 \times 10^3$ km^2/year and 0.4 ± 0.5%/decade) differs from zero by less than one standard deviation and might not be significant.

6. Spatial Distribution of Yearly and Seasonal Trends

The spatial distribution of yearly trends is obtained by applying the BLR technique (Section 3) to the 20-year time series of sea ice concentrations for each of the grid points. The mean sea ice concentration calculated as the mid-point of the 20-year trend is shown in figure 20a. The spatial distribution of the linear trend is shown in 20b, the standard deviation in 20c, and the difference between the 20-year trend and the previously described trends [Gloersen and Mernicky, 1998] for the 8.8-year SMMR time period.

Spatial integration of the trends in concentration in Figure 20b, gives average sector by sector and overall values similar to those for the trends in ice area in Table 7. However, the spatial distribution is not uniform in each sector. The Weddell Sea, Indian Ocean, and W. Pacific Ocean sectors have a predominance of decreases in the outer parts of the ice pack and increases in the inner parts. Most of the Ross Sea sector has increasing trends, and most of the Bellingshausen-Amundsen Seas sector has decreases.

The range of decadal trends from -40% to +32% for the SMMR data [Gloersen and Mernicky, 1998] is reduced to -15% to +11% for the 20-year data (Figure 20b). The differences between the 18.2 -year and 8.8-year decadal trends are shown in Figure 20d. A reversal of trends from

the SMMR data to the 20-year data set is widespread, being the rule rather than the exception (Figure 20d). While this difference map facilitates the location of changes in the trend in the present 20-year period compared to the earlier 8.8-year one, identification of actual trend reversals is more complicated. Positive values of trend differences can indicate either a change from negative in the earlier period to positive in the 20-year period, an increase in positive trend for the longer period, or a decrease in negative trend for the longer period. Of course, all of these situations represent trend increases in the 20-year period. Negative values of the trend differences indicate the opposite.

A notable example of a trend increase is in the vicinity of the former Weddell Polynya [Zwally et al., 1985]. As suggested earlier [Parkinson, 1994, 1998], some regions reveal trend reversals when the 20-year (Figure 21b) and 8.8-year [Gloersen and Mernicky, 1998] trends are compared directly (Figure 20d). The strongest trend reversal is in the W. Pacific near the Ross Sea. During the SMMR years the ice concentration in the eastern portion of the Ross Sea was increasing at a maximum rate of 28-32%/decade, while in the western portion it was decreasing at a maximum rate of 40%. In contrast, during the 20-year period the eastern portion decreased at a maximum rate of about 5%/decade while the western portion increased at a maximum rate of about 11% (Figure 21b). Comparing the shorter (SMMR) and longer (20-year) records of the Weddell Sea reveals more complicated behavior. This region contains both monotonic rate decreases, e.g., in the vicinity of the 1974 Weddell Polynya, as well as trend reversals, e.g., near the Larsen Ice Shelf on the Eastern Antarctic Peninsula the trend was -(8-12)% changing to about +2%. North of the Filchner Ice Shelf (40° W), there was an increase in the positive decadal trend of about 10%. These relatively large local trends average out to a small, but statistically significant, overall increase in the ice concentrations, as indicated by the trend in ice area.

The spatial distribution of the seasonal trends are obtained by applying ordinary least squares (OLS) to each grid element on 2-day intervals by season after removing a modeled seasonal cycle obtained by applying MOLS (Equation (3.1) to the entire data sequence and then using the 10 oscillatory terms as the model. The resulting seasonal means are shown in Figure 21a. and the

decadal trends in Figure 21b. The means differ in some details from the seasonal averages of the SMMR 8.8-year averages by month of the first portion of the present data series shown by Gloersen et al. [1992]. For example, the summer (January-March) composite in Figure 21a shows the outer part of the Western Ross Sea connected by a band of sea ice with about 12-16% concentration, whereas the averages of the first 8.8 years that part of the Ross Sea to be entirely open. Figure 21b shows a significant increasing trend in this area.

Of the seasonal trends shown in Figure 21b, the most negative and positive trends occur in the summer (January-March) with the most positive ones in the eastern Weddell and western Ross Seas, and the most negative ones in the Bellingshausen-Amundsen Seas consistent with the trends in Tables 5 and 7. This pattern persists into the fall (April-June) over larger areas, wut with smaller trends. The Ross Sea is the only sector showing an overall significant increase in all seasons. The Bellingshausen-Amundsen Seas is the only sector showing a decrease in all seasons, although the winter time (July-September) decrease is not significant.

In summer, both the east and west sides of the Antarctic Peninsula are experiencing a reduction in ice cover. Whereas, much of East Antarctica has a significant increase in ice cover near the coast in summer, and in the other three seasons as well. In summer, the ice pack is shifted eastward in the Weddell Sea and westward in the Ross Sea compared to winter. In winter, much of the middle part of the cover in the Weddell Sea has a significant decrease, while the inner and outer parts have an increase. In spring (October-December), the mixed patterns of increasing and decreasing trends are mostly spatially smaller than in the other seasons.

7. Relations Between Changes in Sea Ice and Surface Temperature

Previous analyses of the relationship between Antarctic sea ice variations and seasonal air temperatures [e.g., Weatherly et al., 1991; Jacobs and Comiso, 1993; King, 1994], using temperatures from stations on the continent, showed that sea ice deviations are negatively

correlated with temperatures (i.e., below normal sea ice coverage is associated with above normal temperatures). The ice extent versus temperature correlations were higher and more consistent on a regional basis than for the entire Antarctic. Generally, the correlations were strongest in winter and weakest in summer.

In this study, we use a measurement of the surface temperature over the sea ice covered region to re-examine the sea ice-temperature relationship. Surface temperatures were derived from thermal-infrared satellite data for the months of January and July, as described by Comiso (2000). The satellite infrared data provide a measure of the skin-depth temperature during cloud free conditions. Surface temperature is retrieved separately for open ocean and ice covered regions because of different emissivities of the two surfaces and the difficulty of masking clouds in the latter. A special cloud masking technique had to be developed over ice and snow, as described by Comiso (2000), to reduce the problem of cloud contamination. The temperatures derived from infrared data have been shown to agree with surface air measurements from meteorological stations around the Antarctic continent to within 3 K. This estimate includes the effect of atmospheric inversion, which can be significant in winter, but was minimized as discussed in Comiso (2000). For each of the sectors, the average ice extent is plotted versus the average surface temperature over the ice pack where concentration is $\geq 85\%$, separately for January and July in Figures 22a and 22b along with linear regression fits. An ice concentration threshold of 85% for calculating average surface temperature is used in order to get a better representation of surface ice temperature and hence an approximation to the near-surface air temperature. Residual biases among average ice-ocean surface temperature, ice surface temperature, and near-surface air temperature should have minimal effects on the analysis of correlations between temperature and ice extent.

During winter the slopes of extent versus temperature are all negative (Table 10), indicating less ice with increased temperature. Since sea ice and temperature variations among sectors are generally not in phase, a correlation for total ice can not be obtained directly. However, summation of the correlations for the individual sectors gives an estimated sensitivity for the

total ice pack of - 0.120 ± 0.094 $10^6 km^2/K$ for an overall temperature change. Combining the derived sensitivities of the ice pack to temperature with the observed winter trends from Table 4 gives the implied winter temperature trend (-0. 6 K/decade) that would be consistent with the total sea ice change in winter (+0.4%/decade). In summer, the relationships are less consistent (Table 11), with two sectors (Weddell and W. Pacific) showing a positive correlation of increasing ice with warmer temperatures. The less consistent summer correlation may be partly due to the tendency for melting ice to pin the surface temperature between 0° and -1.8° C, but the data in figure 22 show January average temperatures over the residual ice pack ranging interannually between about -3° and - 8° C. This could be partially due to a bias in the observed temperatures, or maybe an indication that the average temperature in the residual ice pack in January is below melting. The Bellingshausen-Amudsen Sea sector does have a significant negative relation (-12.9 ± 4.0%/K), which is consistent with the findings of Jacobs and Comiso [1993]. In the latter study, the annual average ice extents in the Bellingshausen Sea area were found to correlate very well with annual average surface air temperatures at Rothera station (67.6° S, 68.1° W) in the Antarctic Peninsula with correlation coefficient of -0.77. Also, in Comiso [2000], anomalously warm surface ice temperatures in July in the Bellingshausen Sea (e.g., 1981, 1988, 1989) was found to correspond to considerable retreat in the sea ice cover.

For the 21 Antarctic stations with temperature records longer than 45 years, Comiso [2000] found out that the average trend for the 45-year period (up to 1998) is 0.012 ± 0.014 K/year. Four stations, including the South Pole, have slightly negative trends while the rest have slightly positive trends. A general warming in the Antarctic is confirmed by other studies (e.g., Raper et al., 1984; Jacka and Budd, 1991). However, when data from the last 20 years only is analyzed for direct comparison with satellite data sets, the mean trend was found to be a slight cooling at -0.008 ± 0.016, with 12 stations having negative trends and nine stations with positive trends. Such general cooling during the last 20 years is also suggested by satellite infrared data [Comiso, 2000]. Qualitatively, these results are consistent with trend values shown in Tables 10 and 11.

Table 10. Relations Between Regional Sea Ice Extents and Mean Surface Temperature in Sea Ice Pack for Winter (July 1978 to July 1998)

Regional Sector	Mean Extent in Winter (10^6 x km^2)	Extent/temp Sensitivity ($10^6 km^2/yr/K$)	Extent/temp Sensitivity (%/K)	20-Year Winter Sea Ice Trend (%/decade)	Implied Temp. Trend (K/decade)
Weddell	6.31	- 0.030 ± 0.077	-0.48 ± 1.2	- 0.1 ± 2.3	0.2
Indian	3.11	- 0.040 ± 0.023	-1.29 ± 0.7	- 2.0 ± 2.0	1.6
W. Pacific	1.78	- 0.002 ± 0.027	-0.11 ± 1.5	1.3 ± 3.6	-11.6
Ross	3.84	- 0.030 ± 0.028	-0.78 ± 0.7	3.7 ± 2.5	-4.7
Bell/Amd	2.09	- 0.018 ± 0.022	-0.86 ± 1.1	- 1.2 ± 4.4	1.4
Total	17.14	- 0.120 ± 0.092 (Sum of sectors)	-0.70 ± 0.5	0.4 ± 0.5	-0.6

Table 11. Relations Between Regional Sea Ice Extents and Mean Surface Temperature in Sea Ice Pack for Summer (July 1978 to July 1998)

Regional Sector	Mean Extent in Summer (10^6 x km^2)	Extent/temp Sensitivity ($10^6 km^2/yr/K$)	Extent/temp Sensitivity (%/K)	20-Year Summer Sea Ice Trend (%/decade)	Implied Temp. Trend (K/decade)
Weddell	1.47	0.040 ± 0.042	2.72 ± 2.9	7.7	2.8
Indian	0.30	- 0.009 ± 0.014	- 3.00 ± 4.7	6.0	-2.0
W. Pacific	0.46	0.013 ± 0.023	2.83 ± 5.0	14.5	5.1
Ross	0.99	0.020 ± 0.049	2.02 ± 5.0	12.2	6.0
Bell/Amd	0.70	- 0.090 ± 0.028	- 12.86 ± 4.0	- 32.9	2.6
Total	3.93	- 0.026 ± 0.075 (Sum of sectors)	- 0.66 ± 1.9	2.2	-3.3

8. Effects of the Antarctic Circumpolar Wave

In the sea ice extent curves for the five Antarctic sectors (Figures 3-7), one can visualize the

effects of a wave occasionally influencing a given region, based on a low-frequency wave-like envelope superimposed on the seasonal oscillations. One possibility for a wave-like phenomena is the Antarctic Circumpolar Wave (ACW), characterized by a pattern of wave number 2 and circumpolar migration time of 8 years [White and Petersen, 1996]. Their initial ACW observation has been confirmed more recently with different techniques [Gloersen and Huang, 1999; Gloersen and White, 2001]. Gloersen and Huang [1999] utilized a combination of Complex Singular-Value Decomposition (CSVD) and Empirical Mode Decomposition (EMD) [Huang et al., 1998] to isolate the ACW as residing principally in the quasiquadrennial (QQ) mode separated by the EMD. The Hoffmueller diagram in their Figure 6a clearly depicts several cycles of the ACW. Here, we utilize the data array, which was the basis of their figure, with ice extents in 1° sectors around the South Pole to produce sums of the QQ oscillations in each of 5 sectors (Table 1) as well as the entire pack. These sums are shown in Figure 23 for comparisons with ice extent variations in Figures 2 - 7. Although 5 sectors is not optimum for displaying the characteristics of a wave number 2 pattern, the ACW can be discerned. For example, comparing the results in the Hoffmueller diagram [Gloersen and Huang, 1999] for a persistent ACW trough that begins at 0°E in 1986, in Figure 23 the averaged trough is shown in the Weddell sector also in 1986, in the Indian sector in 1987, in the W. Pacific sector in mid-1988, in the Ross sector in mid-1991, and finally in the B-A sector in 1993.

Although the QQ oscillations associated with the ACW are prominent, the magnitude of their amplitudes ($\lesssim 0.08 \times 10^6$ km^2 peak-to-peak) is only $\approx$ 1/25 compared to the maximum interannual deviations in extent ($\lesssim 2 \times 10^6$ km^2 in Figures 3b-7b). The amplitudes of the QQ oscillations are also only $\approx$ 1/3 compared to the 3 to 5 cycles of interannual variability (amplitudes $\lesssim 0.26 \times 10^6$ km^2), as deduced from the multivariate analysis and shown in table 4 and the fitted cycles in Figures 3b-7b. Therefore, the interannual variability associated with the ACW appears to be only part of the total quasi-periodic interannual variability and small compared to the total interannual variability.

9. Discussion and Conclusions

A primary result of this analysis of the 20 years of measurements of sea ice concentration on the Southern Ocean is the +13,440 ± 4180 km^2/year (+1.18 ± 0.37%/decade) increase in sea ice extent and the +16,960 ± 3,840 km^2/year (+1.96 ± 0.44%/decade) increase in sea ice area. Regionally, the trends in extent are positive in the Weddell Sea (1.5 ± 0.9%/decade), Pacific Ocean (2.4 ± 1.4%/decade), and Ross Sea (6.9 ± 1.1%/decade) sectors, slightly negative in the Indian Ocean (-1.5 ± 1.8%/decade), and negative in the Bellingshausen-Amundsen Seas sector (-9.5 ± 1.5%/decade). An overall increase in Antarctic sea ice cover, during a period when global climate appears to have been warming by 0.2 K/decade [Hansen et al., 1999], stands in marked contrast to the observed decrease in the Arctic sea ice extent of -34,300 ± 3700 km^2/year (-2.8 ± 0.3%/decade) and sea ice area of -29,500 ± 3,800 km^2/year (-2.8 ± 0.4%/decade) in sea ice area [Parkinson et al., 1999]. The observed decrease in the Arctic has been partially attributed to greenhouse warming through climate model simulations with increased CO2 and aerosols [Vinnikov et al., 1999]. As discussed in section 1, an increasing Antarctic sea ice cover is consistent with at least one climate model that includes coupled ice-ocean-atmosphere interactions and a doubling of CO_2 content over 80 years [Manabe et al., 1992].

Another main aspect of the results is the seasonality of the changes, being largest in fall in both magnitude (+26,400 ± 17,400 km^2/year) and fraction (+2.7 ± 1.8%/decade) and second largest in summer (+8,800 ± 12,200 km^2/year and +2.2 ± 3.1%/decade). The changes for the winter season (+7,400 ± 8,500 km^2/year and +0.4 ± 0.5%/decade) and for spring (+10,100 ± 14,000 km^2/year and +0.7 ± 1.0%/decade) are small especially as a fractional change. On a regional basis, the trends differ season to season. During summer and fall, the trends are positive or near zero in all sectors except the Bellingshausen-Amundsen Seas sector. During winter and spring, the trends are negative or near zero in all sectors except the Ross Sea, which has positive trends in all seasons.

In the context of climate change, the sensitivity of the sea ice to changes in temperature is of particular interest. Analysis of the relation between regional sea ice extents and spatially-averaged surface temperatures over the ice pack gives an overall sensitivity between winter ice cover and temperature of - 0.70% change in sea ice extent per K (-0.11 ± 0.09 $10^6 km^2$/K). A change in the winter ice extent of 0.70% corresponds to a latitudinal change in the average

position of ice edge of less than 10 km or a meridional change of less than 0.1 degree which is small compared to some previous estimates (e.g., Parkinson and Bindschadler, 1984). For summer, some regional ice extents vary positively with temperature and others negatively.

The validity of the derived decadal-scale trends depends on two key aspects of this 20-year data set. One is the long-term relative accuracy of the data from multiple satellites with somewhat different sensors and the data processing methodology as described in Cavalieri et al. [1999]. The changes in sea ice cover as small 1%/decade may have climatic significance. This required relative accuracy and long-term data consistency could not have been achieved without the 4 to 6 week periods of overlap from successive satellites, which enabled the algorithm adjustments to make the derived sea ice extents and areas match. Even though the instrumental differences between satellites are small, it has not been possible to understand the differences well enough to provide a satisfactory inter-calibration any other way.

The second key aspect is the complete spatial coverage on daily time scales that allowed the spatial and temporal variability to be adequately quantified in relation to the trends. The characterization of the interannual variability in particular has allowed a calculation of trends that is largely independent of the effects of the periodic components of the variability. In addition, the analysis of data over two decades provides some indication of the interdecadal variability of the sea ice cover and provides a basis for future analysis of continuing observations for inter-decadal changes. Determination of such inter-decadal changes will be particularly important as sea ice changes might accelerate with an increase in climate warming.

The interannual variability of the annual mean sea-ice extent is only 1.6% overall, compared to 5% to 9% in each of five regional sectors. The total variability in the monthly deviations in sea ice extent is 3.4% overall, and from 8 to 15% in the individual sectors. From the first 10 years to the second 10 years, there appears to be a decrease in the variability from 3.9% to 2.7%. Also, there appears to be a decline in the effectiveness in which the anomalies from sector to sector offset each other in the overall spatial average. Analysis of the relative trends in ice extent and ice area imply increases in ice concentration in the W. Pacific and Ross Sea sectors, which could be associated with decreases in variability in those regions.

Although there are significant components of interannual variability with periods of 3 to 5 years, these represent only about 20 to 40% of the total variability in the monthly deviations of the mean. Inclusion of a periodic component in the MOLS gives trends that are considered to be better values than the OLS trends. Nevertheless, the inclusion of about 5 cycles in the 20-year data set and smallness of the periodic amplitudes, minimizes the effect on the calculated linear trends by the OLS method. Therefore, the MOLS and the OLS trends do not differ by more than 0.1σ overall and more than 1σ in the individual sectors.

An interesting aspect of the interannual variability of the seasonal changes is the tendency for periods of greater sea ice extents near the winter maxima to be associated with periods of lesser sea ice extents near the summer minima and vice-versa. In addition, this phenomenen has a period of 3 to 5 years and tends to vary in phase from sector to sector. The phase of the 3 to 5 year periodic components of the interannual variability progresses from sector to sector from the Weddell Sea along East Antarctica, but not consistently through to the Ross Sea sector and Bellingshausen-Amundsen Seas sector. The same effect is shown in Figure 23. While there is an association of the variations with the ACW on a sector to sector basis, the association is not as clear as in the more detailed analysis of extents in 1° longitudinal sectors by Gloersen and Huang [1999].

Acknowledgments: We greatly appreciate the help of John Eylander, Steve Fiegles, Mike Martino, and Jamila Saleh of Raytheon STX for their assistance in the processing of the data and the generation of the figures. We also appreciate the National Snow and Ice Data Center (NSIDC) in Boulder, Colorado, for providing the SSMI radiances. This work was supported by Polar Programs at NASA Headquarters and by NASA's Earth Observing System (EOS) program.

REFERENCES:

Allison, I., The East Antarctic sea ice zone: Ice characteristics and drift, *GeoJournal, 18(1),* 103-115, 1989.

Bjørgo, E., O. M. Johannessen, and M.W. Miles, Analysis of merged SSMR-SSMI time series of Arctic and Antarctic sea ice parameters 1978-1995, *Geophys. Res. Lett., 24(4),* 413-416, 1997.

Bromwich, D. Z. Liu, and A. N. Rogers, Winter atmospheric forcing of the Ross Sea polynya, *Ocean, Ice, and Atmosphere: Interactions at the Antarctic Continental Margin, Antarctic Research Series*, volume 75, ed. by S. S. Jacobs and R. F. Weiss, American Geophysical Union, Washington, D. C., 101-133, 1998.

Carleton, A. M., Antarctic sea-ice relationships with indices of the atmospheric circulation of the Southern Hemisphere, *Clim. Dyn.*, 3, 207-220, 1989.

Carsey, F. D., Microwave observation of the Weddell polynya, *Mon. Weather Rev., 108(12),* 2032-2044, 1980.

Cavalieri, D. J., and S. Martin, A passive microwave study of polynyas along the Antarctic Wilkes Land coast, in *Oceanology of the Antarctic Continental Shelf, Antarctic Research Series*, Volume 43, ed. by S. Jacobs, American Geophysical Union, Washington, D.C., 227-252, 1985.

Cavalieri, D. J., and C. L. Parkinson, Large-scale variations in observed Antarctic sea ice extent and associated atmospheric circulation, *Mon. Weather Rev.*, 109(11), 2323-2336, 1981.

Cavalieri, D. J, P. Gloersen, and W. J. Campbell, Determination of sea ice parameters with the Nimbus 7 SMMR, *J. Geophys. Res.*, 89(D4), 5355-5369, 1984.

Cavalieri, D. J., J. P. Crawford, M. R. Drinkwater, D. T. Eppler, L. D. Farmer, R. R. Jentz, and C. C. Wackerman, Aircraft active and passive microwave validation of sea ice concentration from the Defense Meteorological Satellite Program Special Sensor Microwave Imager, *J. Geophys. Res.*, 96(C12), 21,989-22,008, 1991.

Cavalieri, D. J., K. M. St. Germain, and C. T. Swift, Reduction of weather effects in the calculation of sea-ice concentration with the DMSP SSM/I, *J. Glac.*, 41(139), 455-464, 1995.

Cavalieri, D. J., P. Gloersen, C. L. Parkinson, J. C. Comiso, and H. J. Zwally, Observed hemispheric asymmetry in global sea ice changes, *Science*, 278, 1104-1106, 1997.

Cavalieri, D. J., C. L. Parkinson, P. Gloersen, J. C. Comiso, and H. J. Zwally, Deriving long-term time series of sea ice cover from satellite passive-microwave multisensor data sets, *J. Geophys. Res.*, 104 (C7), 15,803-15,814, 1999.

Comiso, J. C., Characteristics of Arctic winter sea ice from satellite multispectral microwave observations, *J. Geophys. Res., 91*(C1), 975-994, 1986.

Comiso, J. C., *SSM/I Sea Ice Concentrations Using the Bootstrap Algorithm*, NASA Reference Publication 1380, 49 pp., 1995.

Comiso, J. C., Variability and trends in Antarctic surface temperatures from in situ and satellite infrared measurements, *J. Climate, 13(10),* 1674-1696, 2000.

Comiso, J.C., and A.L. Gordon, Cosmonaut polynya in the Southern Ocean: Structure and variability, *J. Geophys. Res., 101(C8),* 18,297-18,313, 1996.

Comiso, J.C., and A.L. Gordon, Interannual variability in summer sea ice minimum, coastal polynyas and bottom water formation in the Weddell Sea, in *Antarctic Sea Ice Physical Properties, Interactions, and Variability, Antarctic Research Series, Volume 74,* ed. by M. O. Jeffries, American Geophysical Union, Washington, D.C., pp.293-315, 1998.

Comiso, J. C., D. J. Cavalieri, C. L. Parkinson, and P. Gloersen, Passive microwave algorithms for sea ice concentration: A comparison of two techniques, *Remote Sens. Environ.,* 60 (3), 357-384, 1997.

Deacon, G.E.R, The hydrology of the Southern Ocean, *Discovery Rep., 15,* 1-124, 1937.

Draper, N. R., and H. Smith, *Applied Regression Analysis,* second edition, 709 pp., John Wiley, New York, 1981.

Enomoto, H., S.-F. Tian, and T. Yamanouchi, Interannual fluctuations of sea ice extent in the Antarctic and associated atmospheric conditions, *Proc. NIPR Symp. Polar Meteorol. Glaciol.,* 6, National Institute of Polar Research, Tokyo, 132-142, 1992.

Fahrbach, E., G. Rohardt, N. Scheele, M. Schröder, V. Strass, and A. Wisotzki, Formation and discharge of deep and bottom water in the northwestern Weddell Sea, *J. Marine Res., 53(4),* 515-538, 1995.

Foster, T. D., and J. H. Middleton, Variability in the bottom water of the Weddell Sea, *Deep-Sea Res., 26A,* 743-762, 1979.

Gloersen, P., and W. J. Campbell, Recent variations in Arctic and Antarctic sea-ice covers, *Nature,* 352, 33-36, 1991.

Gloersen, P., and D. J. Cavalieri, Reduction of weather effects in the calculation of sea ice concentration from microwave radiances, *J. Geophys. Res.*, 91(C3), 3913-3919, 1986.

Gloersen, P., and N. E. Huang, In search of an elusive Antarctic circumpolar wave in sea ice extents: 1978-1996, *Polar Res.*, 18(2), 167-173, 1999.

Gloersen, P., and A. Mernicky, Oscillatory behavior in Antarctic sea ice concentrations, in *Antarctic Sea Ice: Physical Processes, Interactions and Variability, Antarctic Research Series, 74*, ed. by M..O. Jeffries, American Geophysical Union, Washington, D.C., pp.161-171, 1998.

Gloersen P., W. J. Campbell, D. J. Cavalieri, J. C. Comiso, C. L. Parkinson, and H.J. Zwally, Arctic and Antarctic Sea Ice, 1978-1987: Satellite Passive-Microwave Observations and Analysis, *NASA Spec. Publ. 511*, National Aeronautics and Space Administration, Washington, D.C., 1992.

Gloersen P., C. L. Parkinson, D. J. Cavalieri, J. C. Comiso, and H. J. Zwally, Spatial distribution of trends and seasonality in the hemispheric sea ice covers: 1978-1996, *J. Geophys. Res., 104(C9)*, 20,827-20,835, 1999.

Gordon, A. L., and J. C. Comiso, Polynyas in the Southern Ocean, *Scientific American, 256(6),* 90-7, 1988.

Gordon, A.L., B.A. Huber, H.H. Hellmer, and A. Ffield, Deep and bottom water of the Weddell Sea's western rim, *Science, 262*, 95-97, 1993.

Gordon, H. B., and S. P. O'Farrell, Transient climate change in the CSIRO coupled model with dynamic sea ice, *Mon. Weather Rev.*, 125(5), 875-907, 1997.

Hansen, J., R. Ruedy, J. Glascoe, and M. Sato, GISS analysis of surface temperature change, *J. Geophys. Res.*, 104 (D24), 30,997-31,022, 1999.

Huang, N. E., Z. Shen, S. R. Long, M. C. Wu, H. H. Shih, Q. Zheng, N.-C. Yen, C. C. Tung, and H. H. Liu, The empirical mode decomposition and the Hilbert spectrum for nonlinear and non-stationary time series analysis. *Proc. R. Soc. Lond. Ser. A, 454*, 903-995, 1998.

Jacka, T. H., and W. F. Budd, Detection of temperature and sea ice extent changes in the Antarctic and Southern Ocean, *International Conference on the Role of the Polar Regions in Global Change*, ed. by G. Weller, C. L. Wilson, and B. A. B. Severin, vol. 1, 63-70, Geophysical Institute, Univ. Alaska, Fairbanks, 1991.

Jacobs, S. S., and J. C. Comiso, A recent sea-ice retreat west of the Antarctic Peninsula, *Geophys. Res. Letters, 20(12)*, 1171-1174, 1993.

Jacobs, S. S., and J. C. Comiso, Climate variability in the Amundsen and Bellingshausen Seas, *J. Climate, 10(4)*, 697-709, 1997.

Johannessen, O. M., M. Miles, E. Bjørgo, The Arctic's shrinking sea ice, *Nature, 376*, 126-127, 1995.

King, J. C., Recent climate variability in the vicinity of the Antarctic peninsula, *Int. J. Climatol.*, 14, 357-369, 1994.

Kukla, G. J., Recent changes in snow and ice, in *Climatic Change*, ed. by J. Gribbin, Cambridge Univ. Press, London, pp.114-129, 1978.

Kukla, G., and J. Gavin, Summer ice and carbon dioxide, *Science, 214(4520)*, 497-503, 1981.

Kuo, C., C. Lindberg, and D. J. Thomson, Coherence established between atmospheric carbon dioxide and global temperature, *Nature*, 343 (6260), 709-714, 1990.

Lange, M. A., S. F. Ackley, P. Wadhams, G. S. Dieckmann, and H. Eicken, Development of sea ice in the Weddell Sea, *Ann. Glaciol.*, 12, 92-96, 1989.

Lindberg, C. R., Multiple taper spectral analysis of terrestrial free oscillations, Ph.D. thesis, Univ. of Calif., San Diego, 1986.

Lindberg, C. R., and J. Park, Multiple-taper spectral analysis of terrestrial free oscillations: Part II, *Geophys. J. R. Astron. Soc.*, 91(3), 795-836, 1987.

Manabe, S., M. J. Spelman, and R. J. Stouffer, Transient responses of a coupled ocean-atmosphere model to gradual changes of atmospheric CO_2. Part II: Seasonal response, *J. Climate*, 5 (2), 105-126, 1992.

Martinson, D.G., P.D. Killworth, and A.L. Gordon, A convective model for the Weddell Polynya, *J. Phys. Oceanogr.*, 11(4), 466-488, 1981.

NSIDC, DMSP SSM/I Brightness Temperatures and Sea Ice Concentration Grids for the Polar Regions on CD-ROM User's Guide, National Snow and Ice Data Center, *Special Report - 1*, Cooperative Institute for Research in Environmental Sciences, University of Colorado, Boulder, CO, January 1992.

Parkinson, C. L., On the development and cause of the Weddell polynya in a sea ice simulation, *J. Phys. Oceanogr.*, 13(3), 501-511, 1983.

Parkinson, C. L., Spatial patterns in the length of the sea ice season in the Southern Ocean, 1979-1986, *J. Geophys. Res.*, 99(C8), 16,327-16,339, 1994.

Parkinson, C.L., Length of the sea ice season in the southern ocean, 1988-1994, in *Antarctic Sea Ice, Physical Processes, Interactions and Variability, Antarctic Research Series, Volume 74*, ed. by M. O. Jeffries, American Geophysical Union, Washington, D.C., pp. 173-186, 1998.

Parkinson, C. L., and R. A. Bindschadler, Response of Antarctic sea ice to uniform atmospheric temperature increases, in *Climate Processes and Climate Sensitivity*, ed. by J. E. Hansen and T. Takahashi, Maurice Ewing vol. 5, American Geophysical Union, Washington, D.C., 254-264, 1984.

Parkinson, C. L., D. J. Cavalieri, P. Gloersen, H. J. Zwally, and J. C. Comiso, Arctic sea ice extents, areas, and trends, 1978-1996, *J. Geophys. Res*, 104(C9), 20,837-20,856, 1999.

Raper, S.C.B., T.M.L. Wigley, P.R. Mayes, P.D. Jones, and M.J. Salinger, Variations in surface air temperatures. Part 3: The Antarctic, 1957-82. *Mon. Weather Rev.*, **112(7)**, 1341-1353, 1984.

Rintoul, S. R., On the origin and influence of Adélie Land bottom water, *Ocean, Ice, and Atmosphere: Interactions at the Antarctic Continental Margin, Antarctic Research Series*, volume 75, ed. by S. S. Jacobs and R. F. Weiss, American Geophysical Union, Washington, D. C., 151-171, 1998.

Stammerjohn, S.E., and R.C. Smith, Opposing southern ocean climate patterns as revealed by trends in regional sea ice coverage, *Climatic Change, 37*, 617-639, 1997.

Steffen, K., J. Key, D. J. Cavalieri, J. Comiso, P. Gloersen, K. St. Germain, and I. Rubinstein,

The estimation of geophysical parameters using passive microwave algorithms, in *Microwave Remote Sensing of Sea Ice,* ed. by F. Carsey, American Geophysical Union, Washington, D.C., pp.201-231, 1992.

Takizawa, T., K.I. Ohshima, S. Ushio, T. Kawamura, and H. Enomoto, Temperature structure and characteristics appearing on SSM/I images of the Cosmonaut Sea, Antarctica, *Ann. Glaciol.*, 20, 298-306, 1994.

Vinnikov, K. Y., A. Robock, R. J. Stouffer, J. E. Walsh, C. L. Parkinson, D. J. Cavalieri, J. F. B. Mitchell, D. Garrett, and V. F. Zakharov, Global warming and Northern Hemisphere sea ice extent, *Science* 286, 1934-1937, 1999.

Wakatsuchi, M., K.I. Ohshima, M. Hishida, and M. Naganobu, Observations of a street of cyclonic eddies in the Indian Ocean sector of the Antarctic Divergence, *J. Geophys. Res.*, 99(C10), 20,417-20,426, 1994.

Watkins, A. B., and I. Simmonds, Current trends in Antarctic sea ice: The 1990s impact on a short climatology, *J. Climate*, 13, 4441-4451, 2000.

Weatherly, J. W., J. E. Walsh, and H. J. Zwally, Antarctic sea ice variations and seasonal air temperature relationships, *J. Geophys. Res.*, 96 (C8), 15,119-15,130, 1991.

White, W. B., and R. G. Peterson, An Antarctic circumpolar wave in surface pressure, wind, temperature and sea-ice extent, *Nature, 380(6576),* 699-702, 1996.

Worby, A.P., R.A. Massom, I. Allison, V.I. Lytle, and P. Heil, East Antarctic sea ice: A review of its structure, properties and drift, in *Antarctic Sea Ice: Physical Properties, Interactions and Variability, Antarctic Research Series, Volume 74,* ed. by M. O. Jeffries, American Geophysical Union, Washington, D. C., pp.41-67, 1998.

Zwally, H. J., and P. Gloersen, Passive microwave images of the polar regions and research applications, *Polar Record*, 18 (116), 431-450, 1977.

Zwally, H. J., C. L. Parkinson, and J. C. Comiso, Variability of Antarctic sea ice and changes in carbon dioxide, *Science*, 220 (4601), 1005-1012, 1983a.

Zwally, H. J., J. C. Comiso, C. L. Parkinson, W. J. Campbell, F. D. Carsey, and P. Gloersen, Antarctic Sea Ice, 1973-1976: Satellite Passive-Microwave Observations, *NASA Spec. Publ. 459*, National Aeronautics and Space Administration, Washington, D.C., 1983b.

Zwally, H. J., J. C. Comiso, and A. L. Gordon, Antarctic offshore leads and polynyas and oceanographic effects, in *Oceanology of the Antarctic Continental Shelf*, Antarctic Research Series, Volume 43, ed. by S. Jacobs, American Geophysical Union, Washington, D.C., 203-226, 1985.

List of Figures:

Figure 1. Average sea ice concentration maps averaged over the first 10 years (1979 - 1988) and the second 10 years (1989 - 1998) and their differences for a) the month of summer minimum and b) September, the month of winter maximum. The five regional sectors are Weddell Sea (60° W to 20° E), Indian Ocean (20° E to 90° E), Pacific Ocean (90° E to 160° E), Ross Sea (160° E to 140° W), and Bellingshausen-Amundsen Seas (140° W to 60° W).

Figure 2. Time series of Antarctic sea ice sea extent for total Southern Ocean from November 1978 through December 1998. (a) monthly-averages showing the seasonal cycle averaged over the 20 years in inset, (b) monthly deviations from the 20-year monthly-averaged values (e.g. January 1978 minus the 20-year January mean), and the multivariate linear trend and sinusoidal fit with an interannual period 3 years superimposed on the deviations (other figures use 3, 4, or 5 years depending on which period gave the largest amplitude in the fit to sea ice extent). (c) yearly and seasonally averages plus the least squares linear trend line. Summer values (Su) are averages for January-March, Autumn (A) for April-June, Winter values (W) for July-September, and spring (Sp) for October-December.

Figure 3. Time series of Antarctic sea ice sea extent for Weddell Sea sector, similar to Figure 2.

Figure 4. Time series of sea ice sea extent for Indian Ocean sector, similar to Figure 2.

Figure 5. Time series of sea ice sea extent for Western Pacific Ocean sector. sector, similar to Figure 2.

Figure 6. Time series of sea ice sea extent for Ross Sea sector, similar to Figure 2.

Figure 7. Time series of sea ice sea extent for Bellingshausen/Amundsen Seas sector, similar to Figure 2.

Figure 8. Time series of Antarctic sea ice area with C ≥ 15% for total Southern Ocean from November 1978 through December 1998, similar to Figure 2.

Figure 9. Time series of sea ice area with C ≥ 15% for Weddell Sea sector, similar to Figure 8.

Figure 10. Time series of sea ice area with C ≥ 15% for Indian Ocean sector, similar to Figure 8.

Figure 11. Time series of sea ice area with C ≥ 15% for Western Pacific Ocean sector, similar to Figure 8.

Figure 12. Time series of sea ice area with C ≥ 15% for Ross Sea sector, similar to Figure 8.

Figure 13. Time series of sea ice area with C ≥ 15% for Bellingshausen/Amundsen Seas sector, similar to Figure 8.

Figure 14. Time series of open water area within Antarctic ice pack for total Southern Ocean from November 1978 through December 1998, similar to Figure 2.

Figure 15. Time series of open water area within ice pack for Weddell Sea sector, similar to Figure 14.

Figure 16. Time series of open water area within ice pack for Indian Ocean sector, similar to Figure 14.

Figure 17. Time series of open water area within ice pack for Western Pacific Ocean sector, similar to Figure 14.

Figure 18. Time series of open water area within ice pack for Ross Sea sector, similar to Figure 14.

Figure 19. Time series of open water area within ice pack for Bellingshausen/Amundsen Seas sector, similar to Figure 14.

Figure 20. Spatial distribution of yearly trends from application of band-limited regression (BLR) to each grid element of maps of sea ice concentration record on 2-day intervals for 20 years. a) The 20-year mean sea ice concentration, b) the decadal trend in concentration, c) the standard deviation of the decadal trend, and d) differences between the 20-year and 1978-1987 trends.

Figure 21. Spatial distribution of seasonal trends from application of ordinary least squares regression (OLS) to each grid element of of maps of sea ice concentration record on 2-day intervals for 20 years after subtracting the model seasonal cycle (with coefficients determined by multiple ordinary least squares regression, MOLSR). a) The 20-year mean sea ice concentration by season, and b) the decadal trend in concentration by season.

Figure 22. Relations between regionally-averaged sea ice extents and regionally-averaged surface temperatures over the ice pack as derived from satellite infrared for a) summer month of January showing generally in consistent relations from sector to sector, and b) winter month of July showing negative relations between sea ice extents and temperature.

Figure 23. Quasiquadrennial (QQ) modes of the sea ice concentration oscillations by regional sector. These QQ modes are obtained by summing over the regional sectors the results of the Empirical Mode Decomposition of sea ice concentrations in 1° longitudinal sectors around the pole by Gloersen and Huang [1999].

(a)

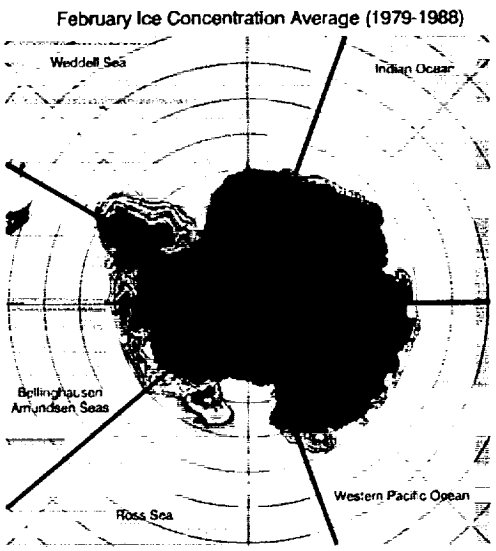
February Ice Concentration Average (1979-1988)
Weddell Sea
Indian Ocean
Bellingshausen
Amundsen Seas
Western Pacific Ocean
Ross Sea

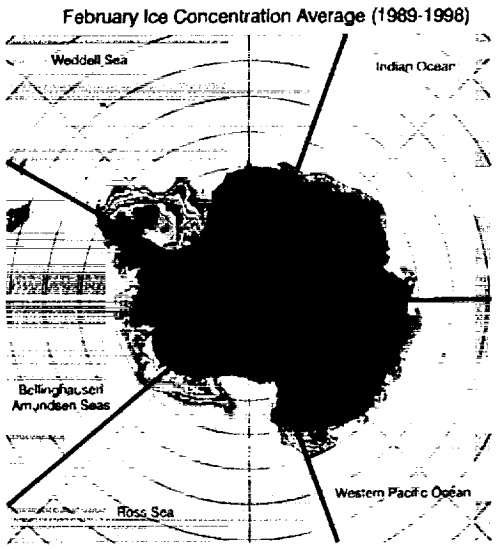
February Ice Concentration Average (1989-1998)
Weddell Sea
Indian Ocean
Bellingshausen
Amundsen Seas
Western Pacific Ocean
Ross Sea

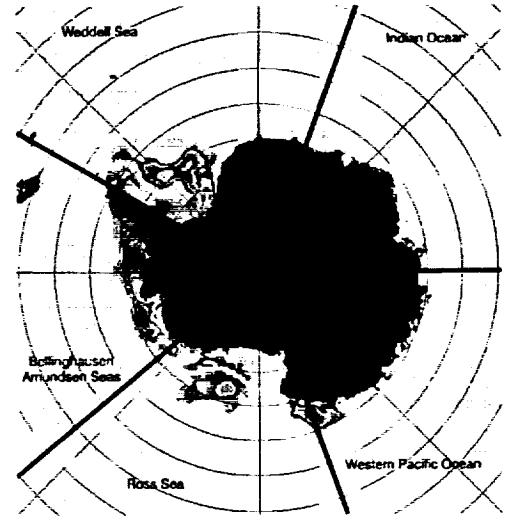
February Average (1989-1998) - February Average (1979-1988)
Weddell Sea
Indian Ocean
Bellingshausen
Amundsen Seas
Western Pacific Ocean
Ross Sea

(b)

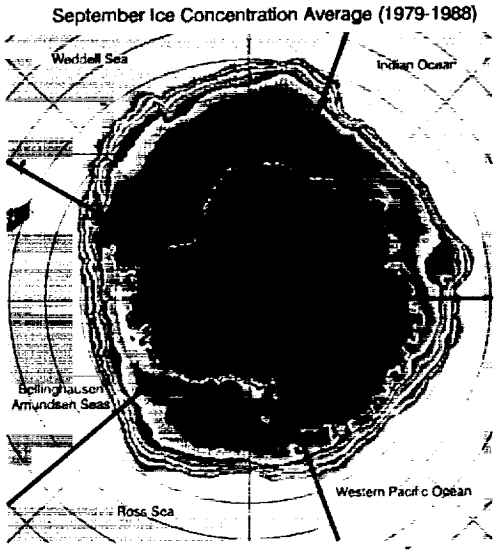
September Ice Concentration Average (1979-1988)
Weddell Sea
Indian Ocean
Bellingshausen
Amundsen Seas
Western Pacific Ocean
Ross Sea

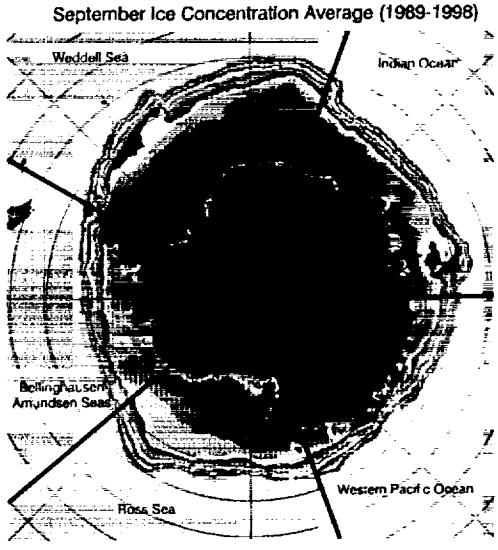
September Ice Concentration Average (1989-1998)
Weddell Sea
Indian Ocean
Bellingshausen
Amundsen Seas
Western Pacific Ocean
Ross Sea

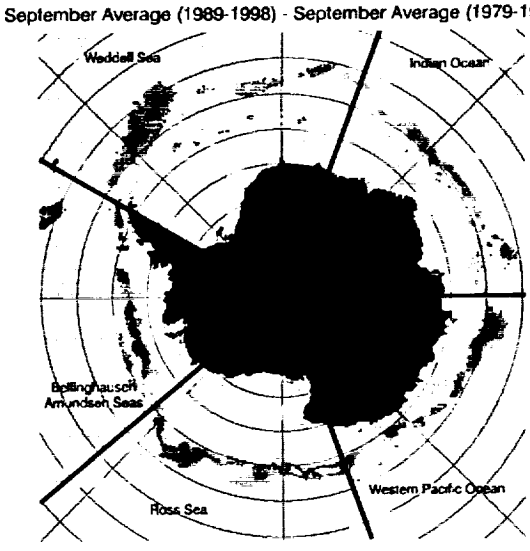
September Average (1989-1998) - September Average (1979-1988)
Weddell Sea
Indian Ocean
Bellingshausen
Amundsen Seas
Western Pacific Ocean
Ross Sea


>=96%
96%
92%
88%
84%
80%
76%
72%
68%
64%
60%
56%
52%
48%
44%
40%
36%
32%
28%
24%
20%
16%
12%
>=55
55
50
45
40
35
30
25
20
15
10
5
0
-5
-10
-15
-20
-25
-30
-35
-40
-45
-50
-55

Figure 1

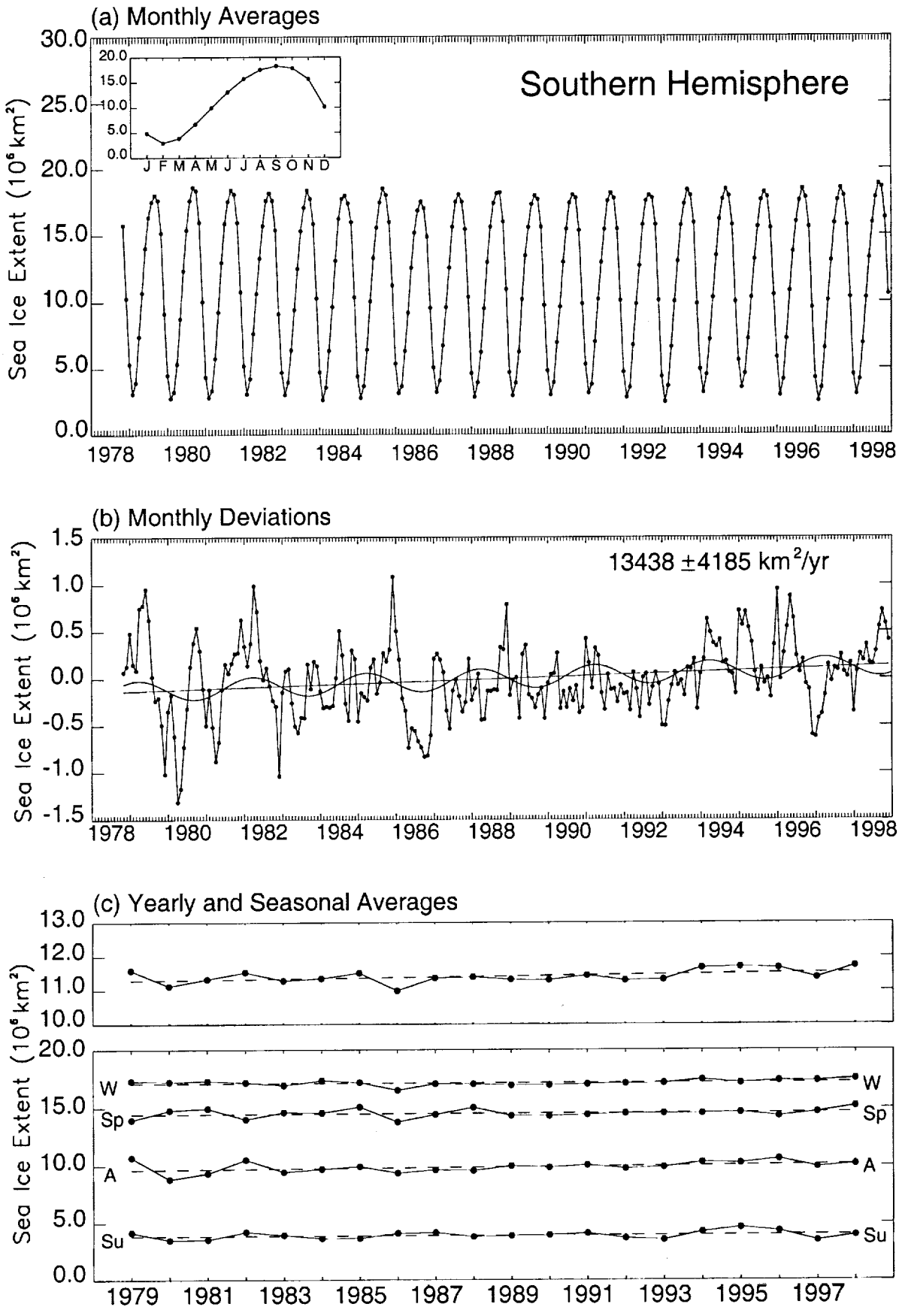
(a) Monthly Averages
Southern Hemisphere
Sea Ice Extent (10^6 km^2)
30.0
25.0
20.0
15.0
10.0
5.0
0.0
1978 1980 1982 1984 1986 1988 1990 1992 1994 1996 1998
J F M A M J J A S O N D
(b) Monthly Deviations
13438 ±4185 km^2/yr
1.5
1.0
0.5
0.0
-0.5
-1.0
-1.5
(c) Yearly and Seasonal Averages
13.0
12.0
11.0
10.0
W
Sp
A
Su
1979 1981 1983 1985 1987 1989 1991 1993 1995 1997

Figure 2.

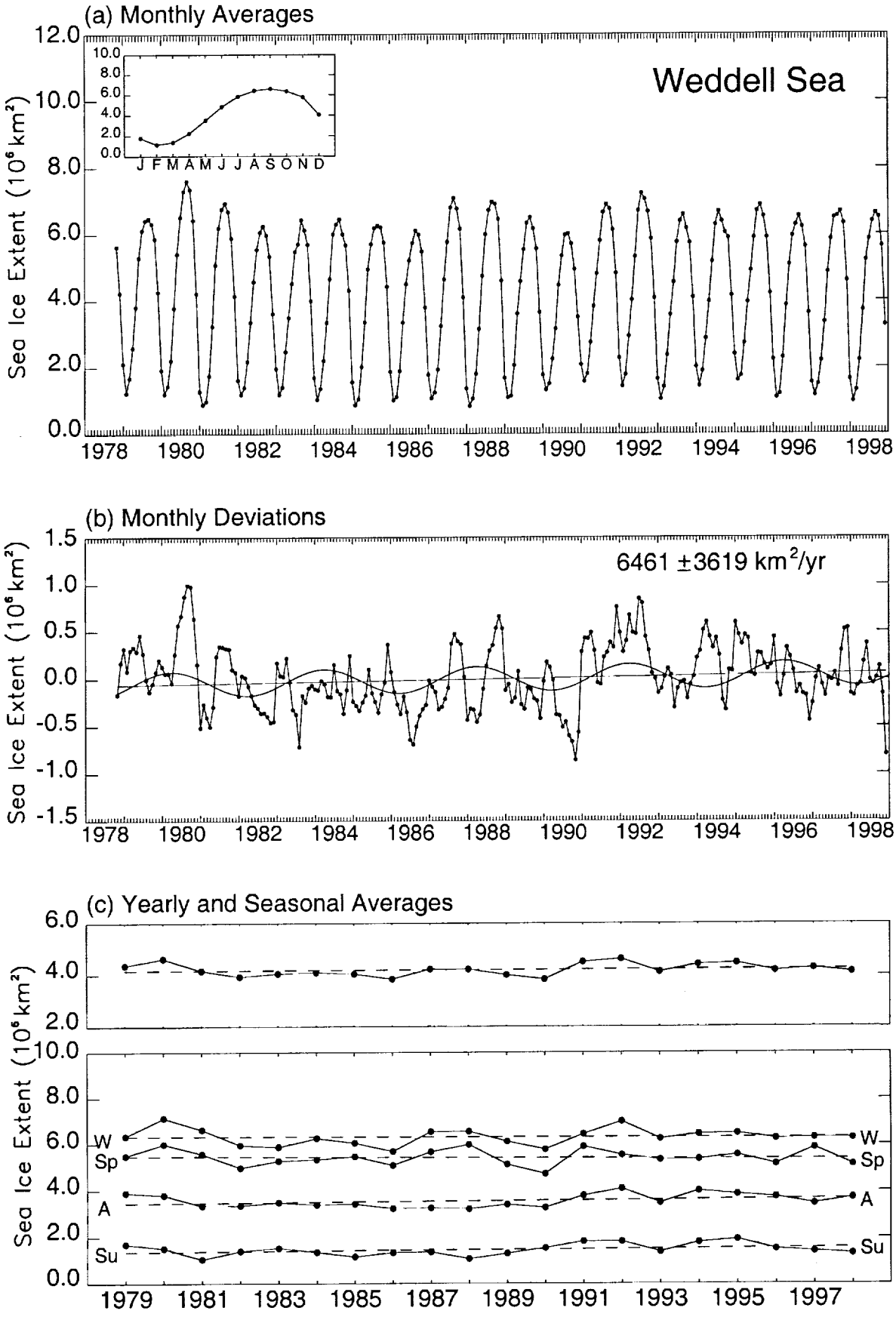
(a) Monthly Averages
Weddell Sea
Sea Ice Extent (10^6 km^2)
J F M A M J J A S O N D
(b) Monthly Deviations
6461 ±3619 km^2/yr
(c) Yearly and Seasonal Averages
W
Sp
A
Su
1978 1980 1982 1984 1986 1988 1990 1992 1994 1996 1998
1979 1981 1983 1985 1987 1989 1991 1993 1995 1997

Figure 3.

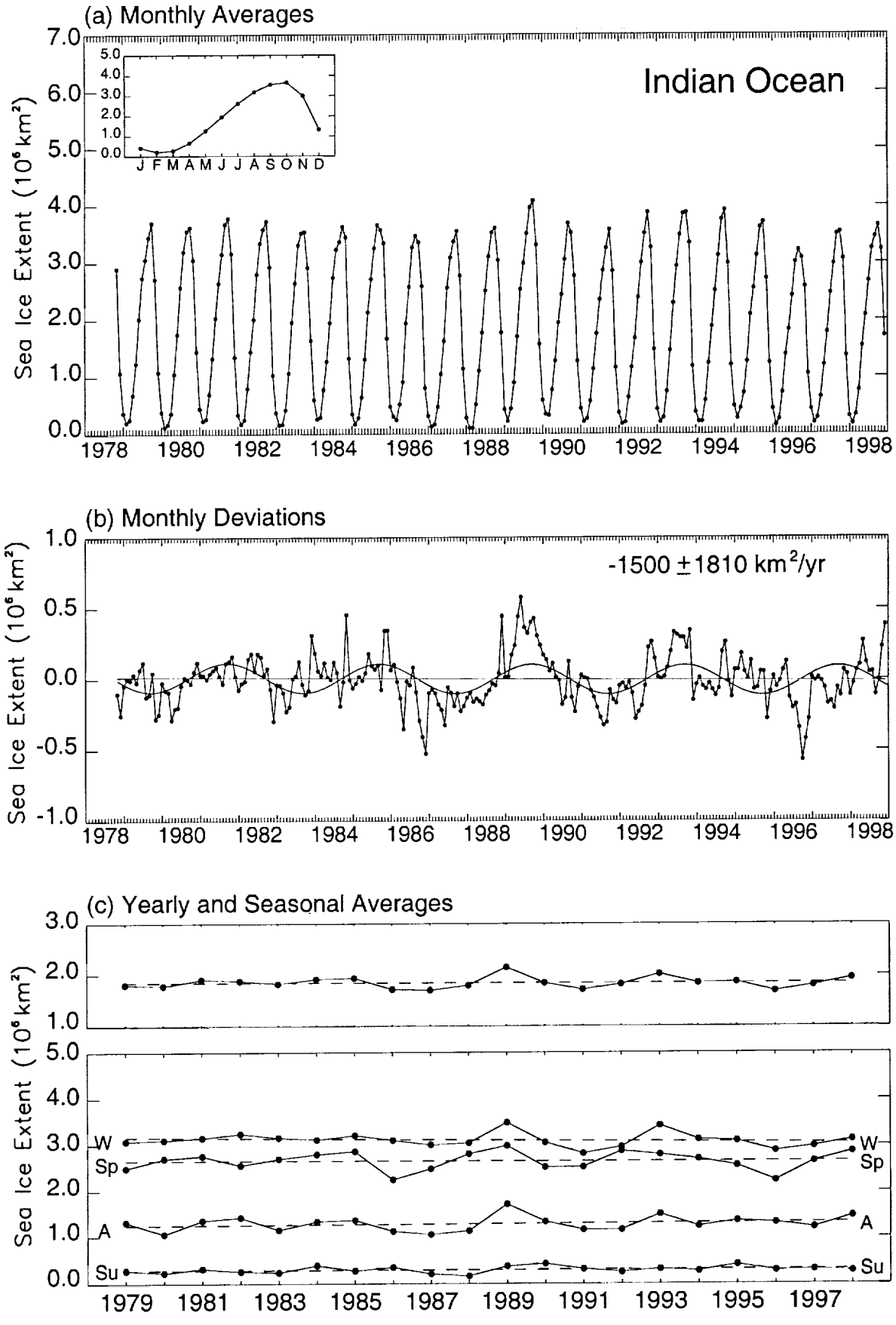
(a) Monthly Averages
Indian Ocean
Sea Ice Extent (10^6 km^2)
7.0
6.0
5.0
4.0
3.0
2.0
1.0
0.0
1978 1980 1982 1984 1986 1988 1990 1992 1994 1996 1998
5.0
4.0
3.0
2.0
1.0
0.0
J F M A M J J A S O N D
(b) Monthly Deviations
-1500 ±1810 km^2/yr
Sea Ice Extent (10^6 km^2)
1.0
0.5
0.0
-0.5
-1.0
1978 1980 1982 1984 1986 1988 1990 1992 1994 1996 1998
(c) Yearly and Seasonal Averages
Sea Ice Extent (10^6 km^2)
3.0
2.0
1.0
5.0
4.0
3.0
2.0
1.0
0.0
W
Sp
A
Su
1979 1981 1983 1985 1987 1989 1991 1993 1995 1997

Figure 4.

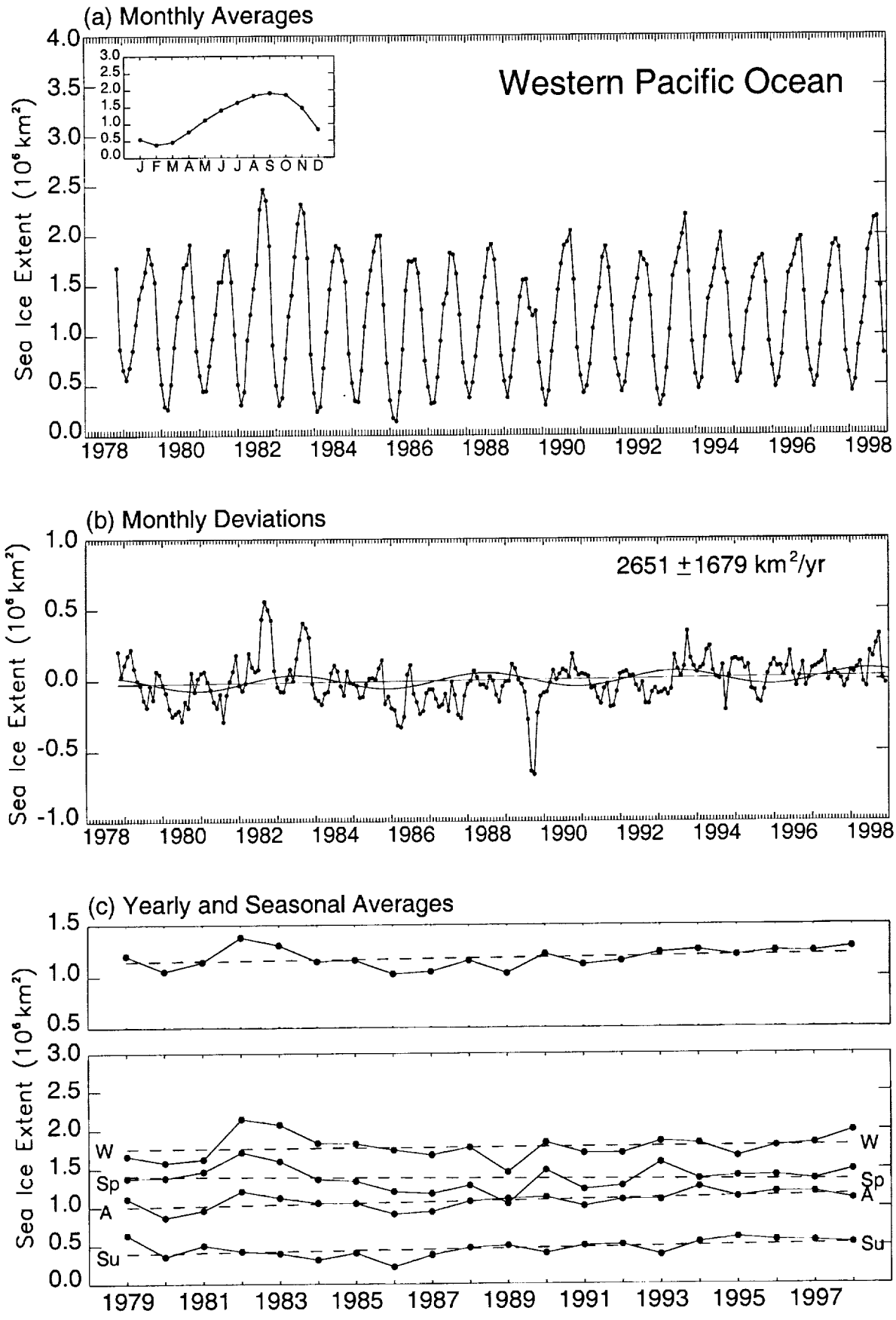
(a) Monthly Averages
Western Pacific Ocean
Sea Ice Extent (10^6 km^2)
J F M A M J J A S O N D
(b) Monthly Deviations
2651 ±1679 km^2/yr
(c) Yearly and Seasonal Averages
W
Sp
A
Su
1978 1980 1982 1984 1986 1988 1990 1992 1994 1996 1998
1979 1981 1983 1985 1987 1989 1991 1993 1995 1997

Figure 5

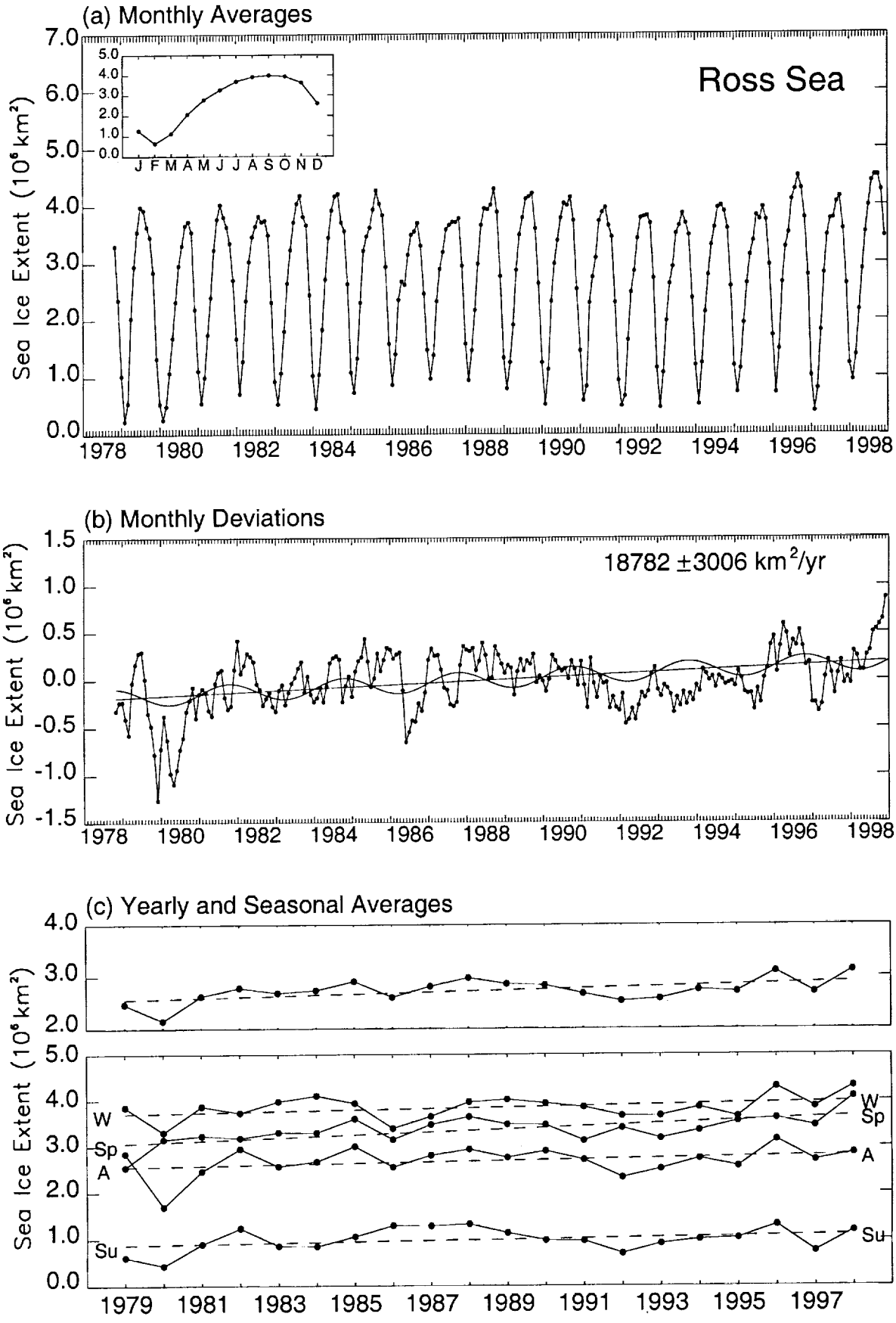
(a) Monthly Averages
Ross Sea
Sea Ice Extent (10^6 km^2)
7.0
6.0
5.0
4.0
3.0
2.0
1.0
0.0
5.0
4.0
3.0
2.0
1.0
0.0
J F M A M J J A S O N D
1978 1980 1982 1984 1986 1988 1990 1992 1994 1996 1998
(b) Monthly Deviations
18782 ±3006 km^2/yr
Sea Ice Extent (10^6 km^2)
1.5
1.0
0.5
0.0
-0.5
-1.0
-1.5
1978 1980 1982 1984 1986 1988 1990 1992 1994 1996 1998
(c) Yearly and Seasonal Averages
Sea Ice Extent (10^6 km^2)
4.0
3.0
2.0
5.0
4.0
3.0
2.0
1.0
0.0
W
Sp
A
Su
1979 1981 1983 1985 1987 1989 1991 1993 1995 1997

Figure 6.

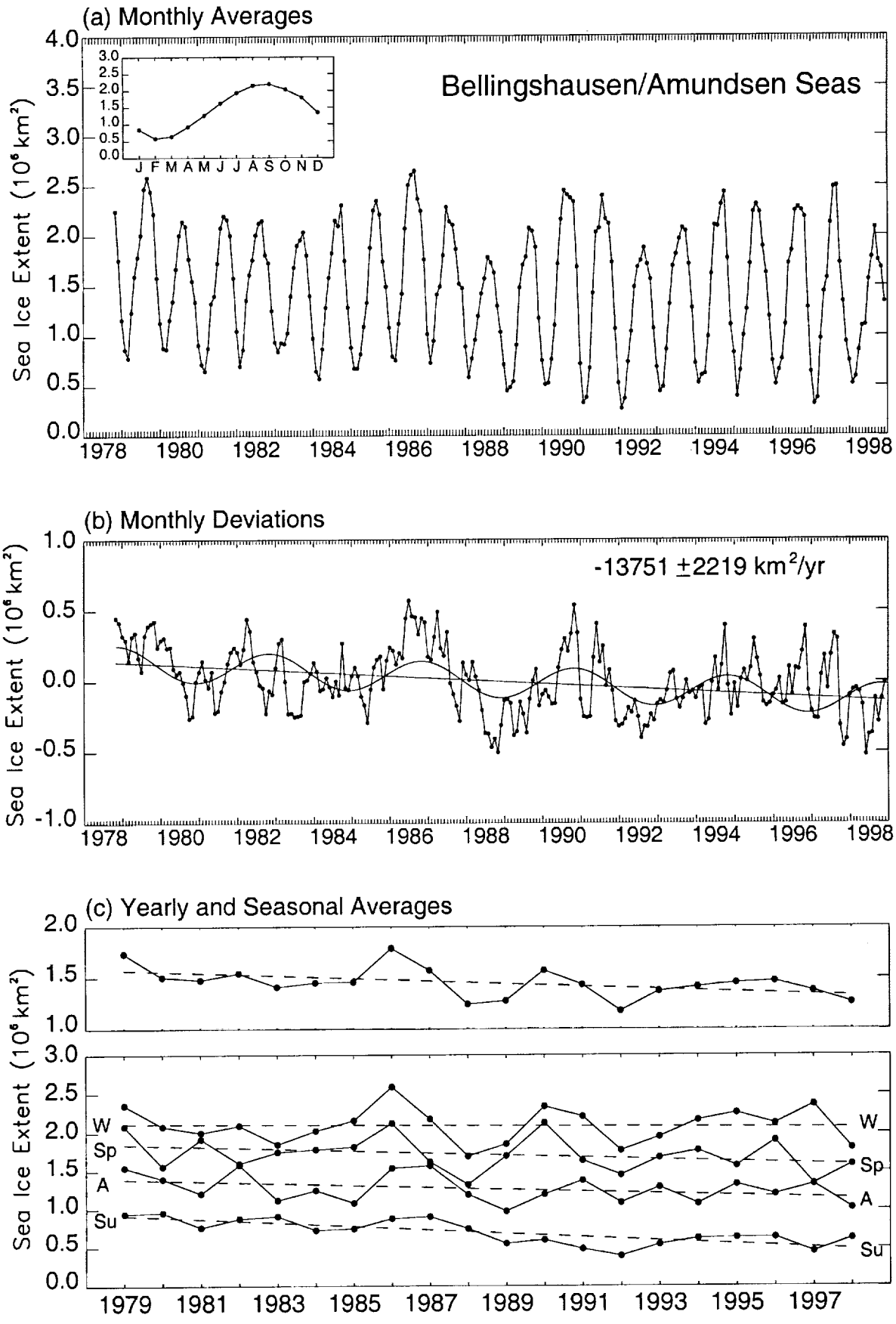
(a) Monthly Averages
Bellingshausen/Amundsen Seas
Sea Ice Extent (10^6 km^2)
J F M A M J J A S O N D
(b) Monthly Deviations
-13751 ±2219 km^2/yr
Sea Ice Extent (10^6 km^2)
(c) Yearly and Seasonal Averages
Sea Ice Extent (10^6 km^2)
W
Sp
A
Su

Figure 7.

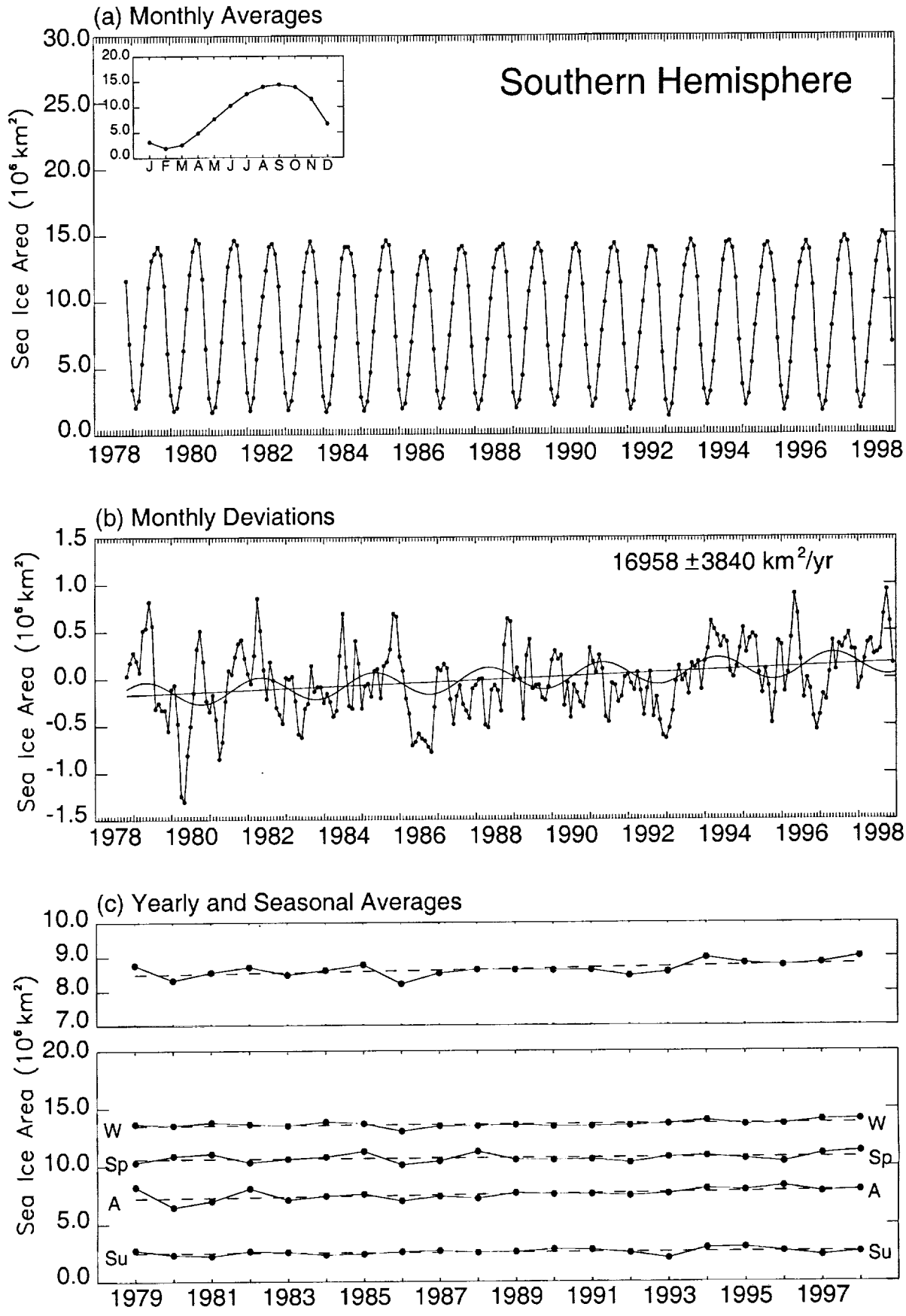
(a) Monthly Averages
Southern Hemisphere
Sea Ice Area (10^6 km^2)
30.0
25.0
20.0
15.0
10.0
5.0
0.0
20.0
15.0
10.0
5.0
0.0
J F M A M J J A S O N D
1978 1980 1982 1984 1986 1988 1990 1992 1994 1996 1998
(b) Monthly Deviations
16958 ±3840 km^2/yr
Sea Ice Area (10^6 km^2)
1.5
1.0
0.5
0.0
-0.5
-1.0
-1.5
1978 1980 1982 1984 1986 1988 1990 1992 1994 1996 1998
(c) Yearly and Seasonal Averages
Sea Ice Area (10^6 km^2)
10.0
9.0
8.0
7.0
20.0
15.0
10.0
5.0
0.0
W
Sp
A
Su
1979 1981 1983 1985 1987 1989 1991 1993 1995 1997

Figure 8.

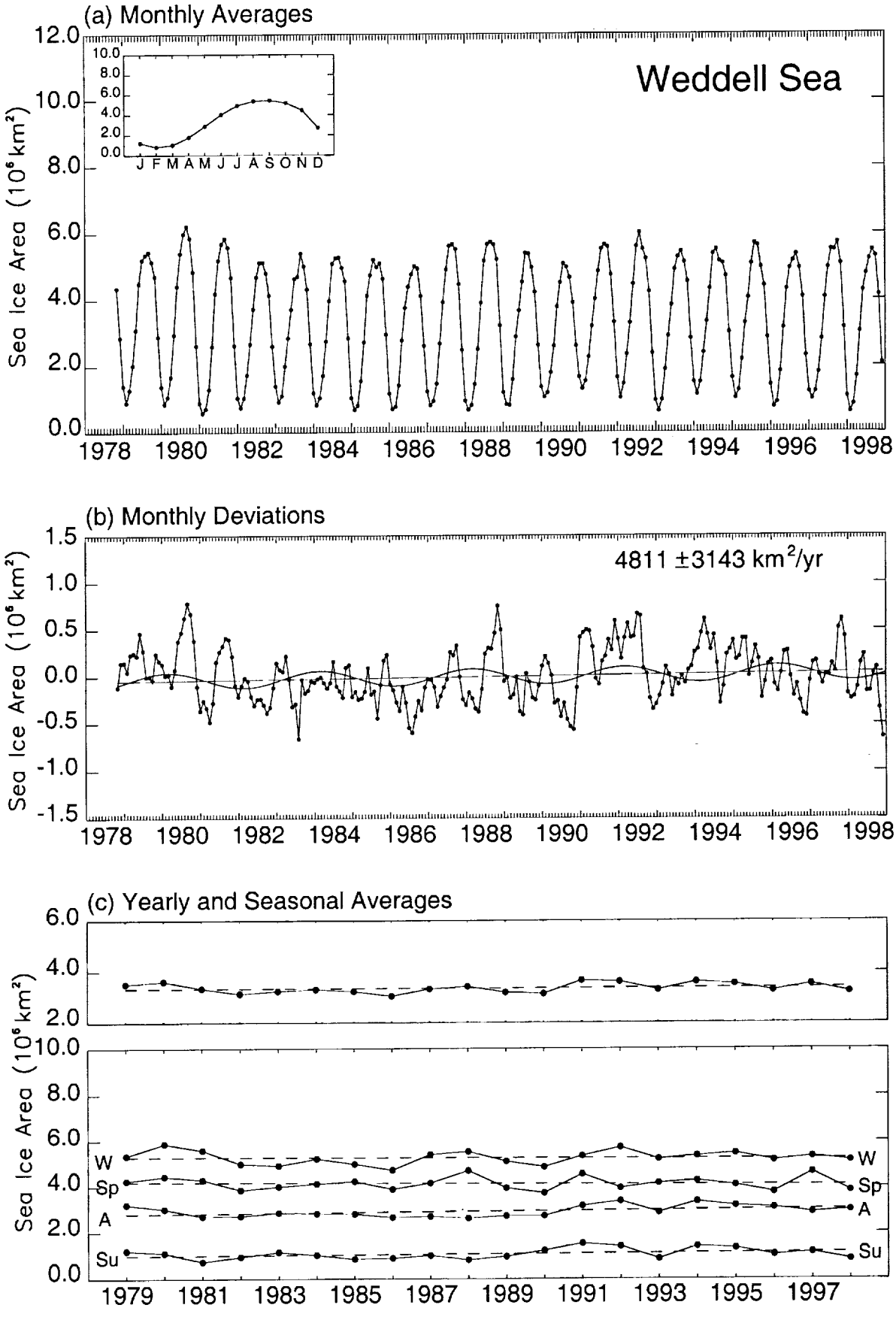
(a) Monthly Averages
Weddell Sea
Sea Ice Area (10^6 km^2)
12.0
10.0
8.0
6.0
4.0
2.0
0.0
J F M A M J J A S O N D
1978 1980 1982 1984 1986 1988 1990 1992 1994 1996 1998
(b) Monthly Deviations
4811 ±3143 km^2/yr
1.5
1.0
0.5
0.0
-0.5
-1.0
-1.5
(c) Yearly and Seasonal Averages
W
Sp
A
Su
1979 1981 1983 1985 1987 1989 1991 1993 1995 1997

Figure 9.

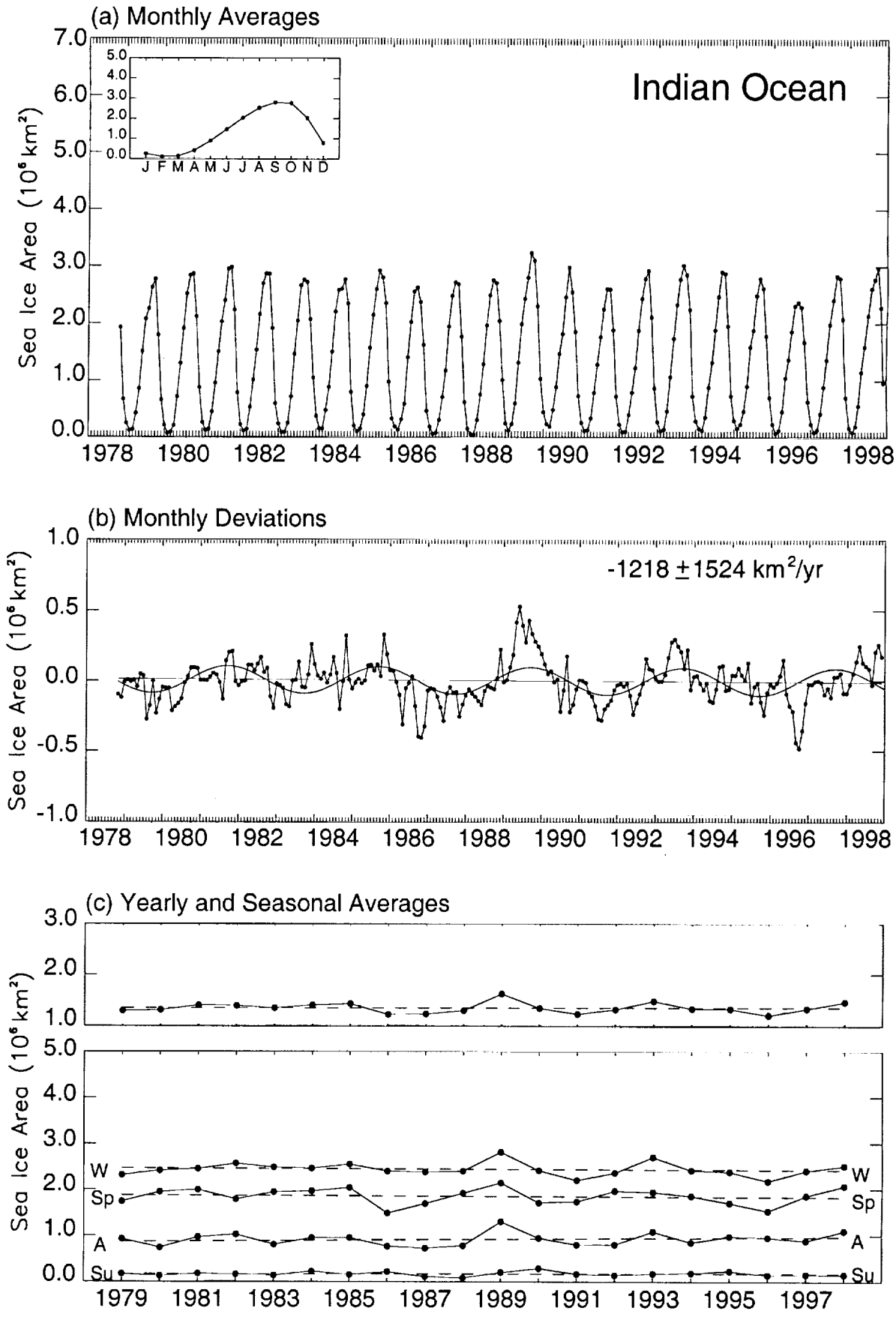
(a) Monthly Averages
Indian Ocean
Sea Ice Area (10^6 km^2)
7.0
6.0
5.0
4.0
3.0
2.0
1.0
0.0
1978 1980 1982 1984 1986 1988 1990 1992 1994 1996 1998
J F M A M J J A S O N D
(b) Monthly Deviations
-1218 ±1524 km^2/yr
1.0
0.5
0.0
-0.5
-1.0
(c) Yearly and Seasonal Averages
W
Sp
A
Su
1979 1981 1983 1985 1987 1989 1991 1993 1995 1997

Figure 10.

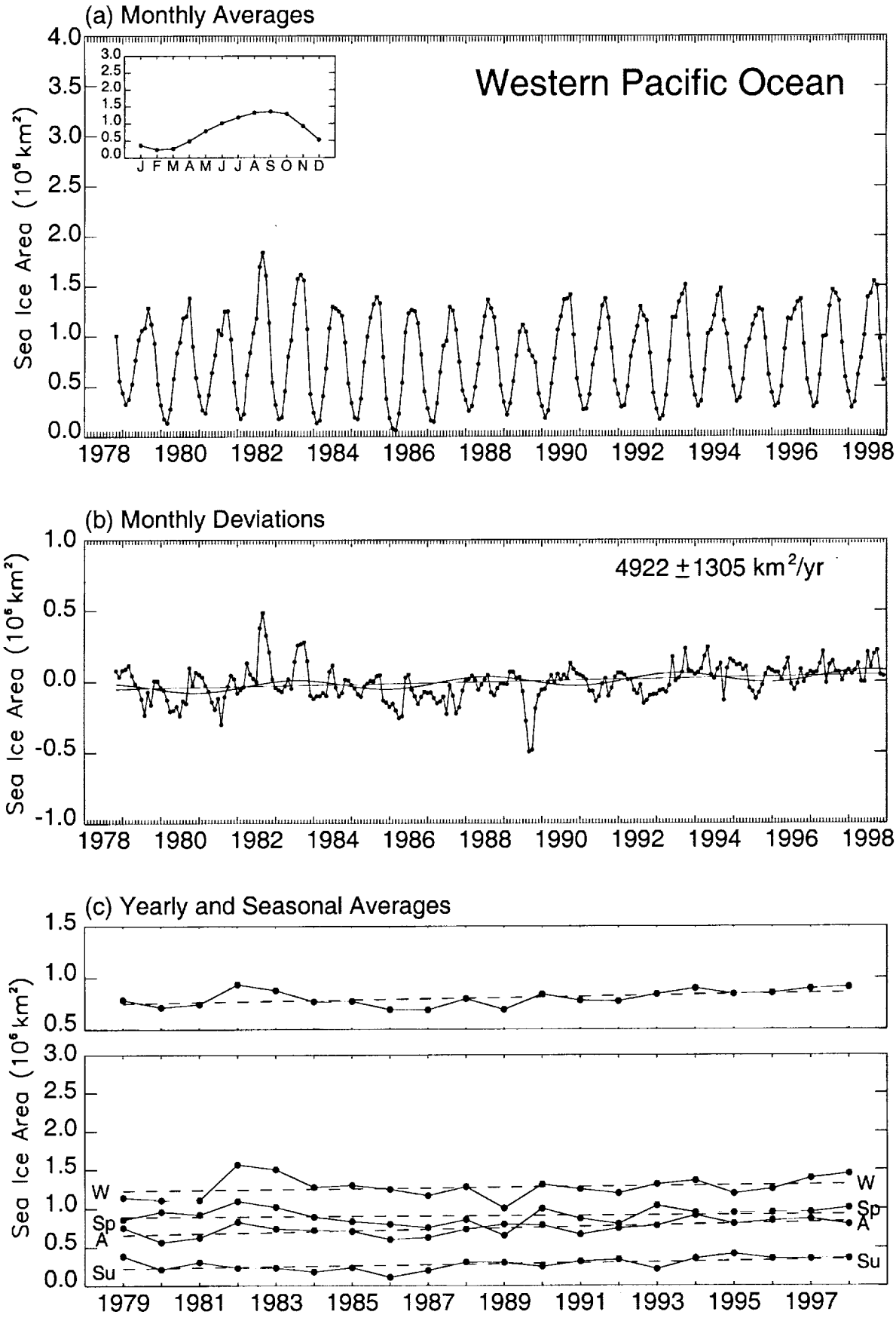
(a) Monthly Averages
Western Pacific Ocean
Sea Ice Area (10^6 km^2)
J F M A M J J A S O N D
(b) Monthly Deviations
4922 ±1305 km^2/yr
(c) Yearly and Seasonal Averages
W
Sp
A
Su

Figure 11

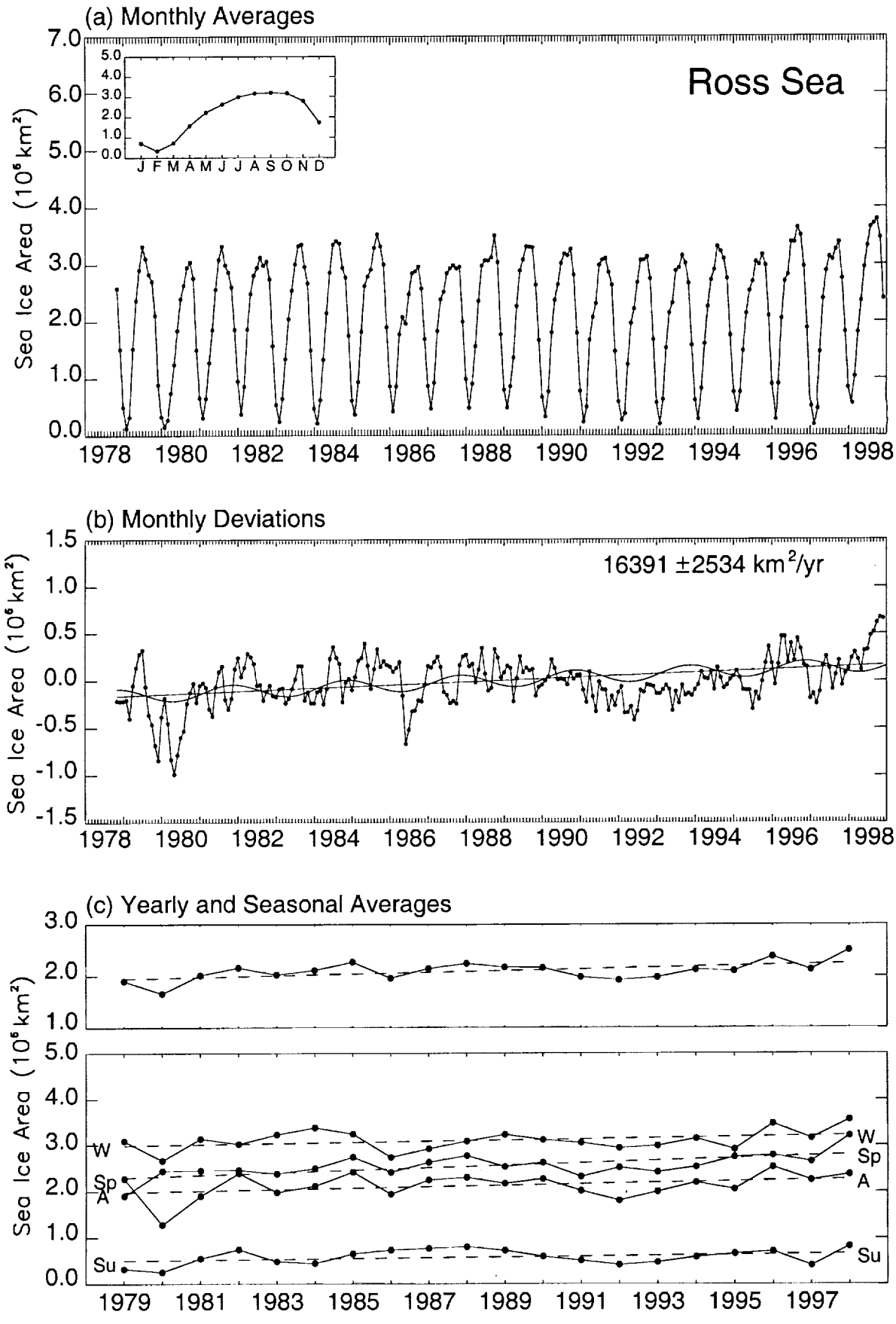
(a) Monthly Averages
Ross Sea
Sea Ice Area (10^6 km^2)
J F M A M J J A S O N D
1978 1980 1982 1984 1986 1988 1990 1992 1994 1996 1998
(b) Monthly Deviations
16391 ±2534 km^2/yr
Sea Ice Area (10^6 km^2)
1978 1980 1982 1984 1986 1988 1990 1992 1994 1996 1998
(c) Yearly and Seasonal Averages
Sea Ice Area (10^6 km^2)
W
Sp
A
Su
1979 1981 1983 1985 1987 1989 1991 1993 1995 1997

Figure 12.

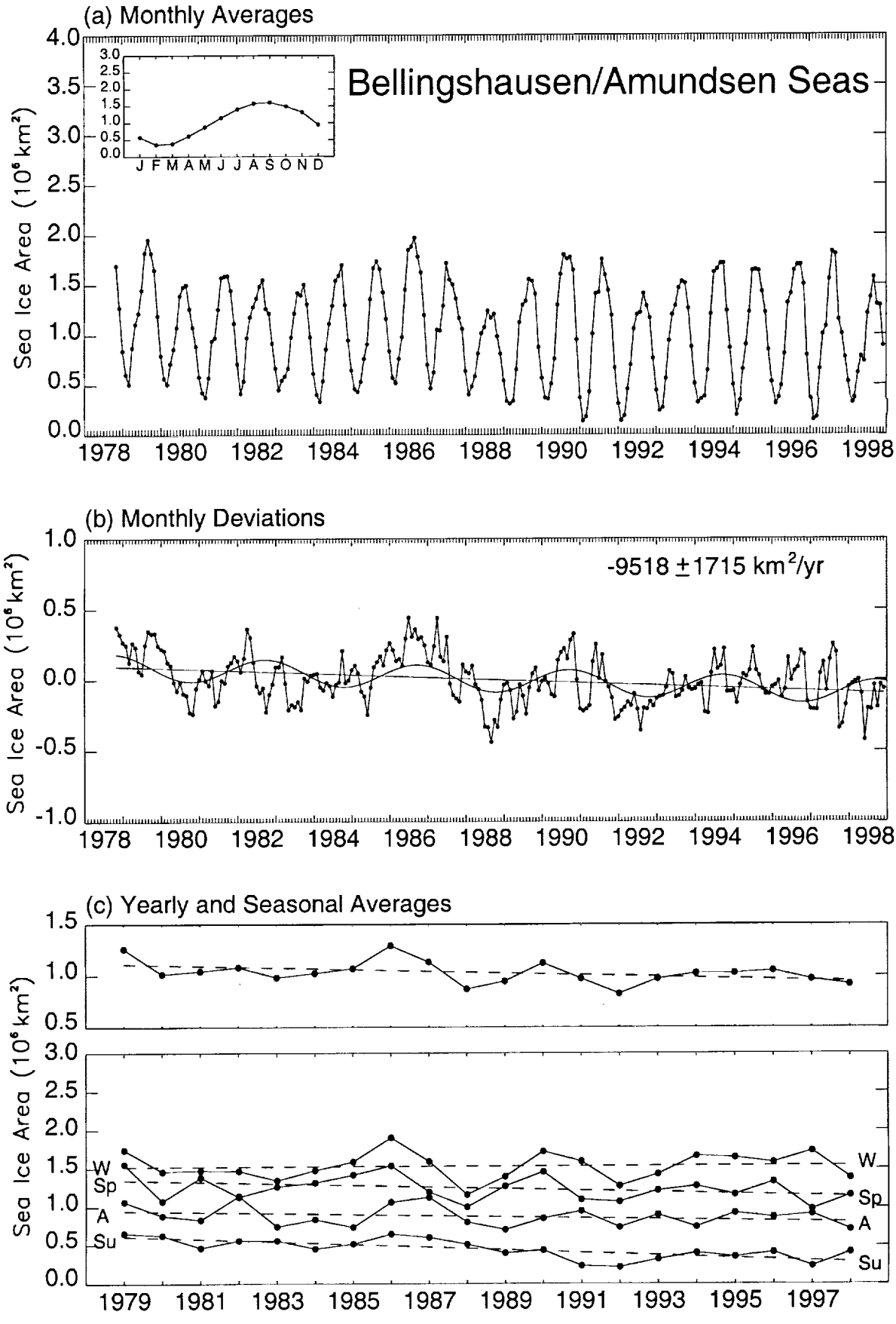
(a) Monthly Averages
Bellingshausen/Amundsen Seas
Sea Ice Area (10^6 km^2)
J F M A M J J A S O N D
(b) Monthly Deviations
-9518 ±1715 km^2/yr
(c) Yearly and Seasonal Averages
W
Sp
A
Su

Figure 13.

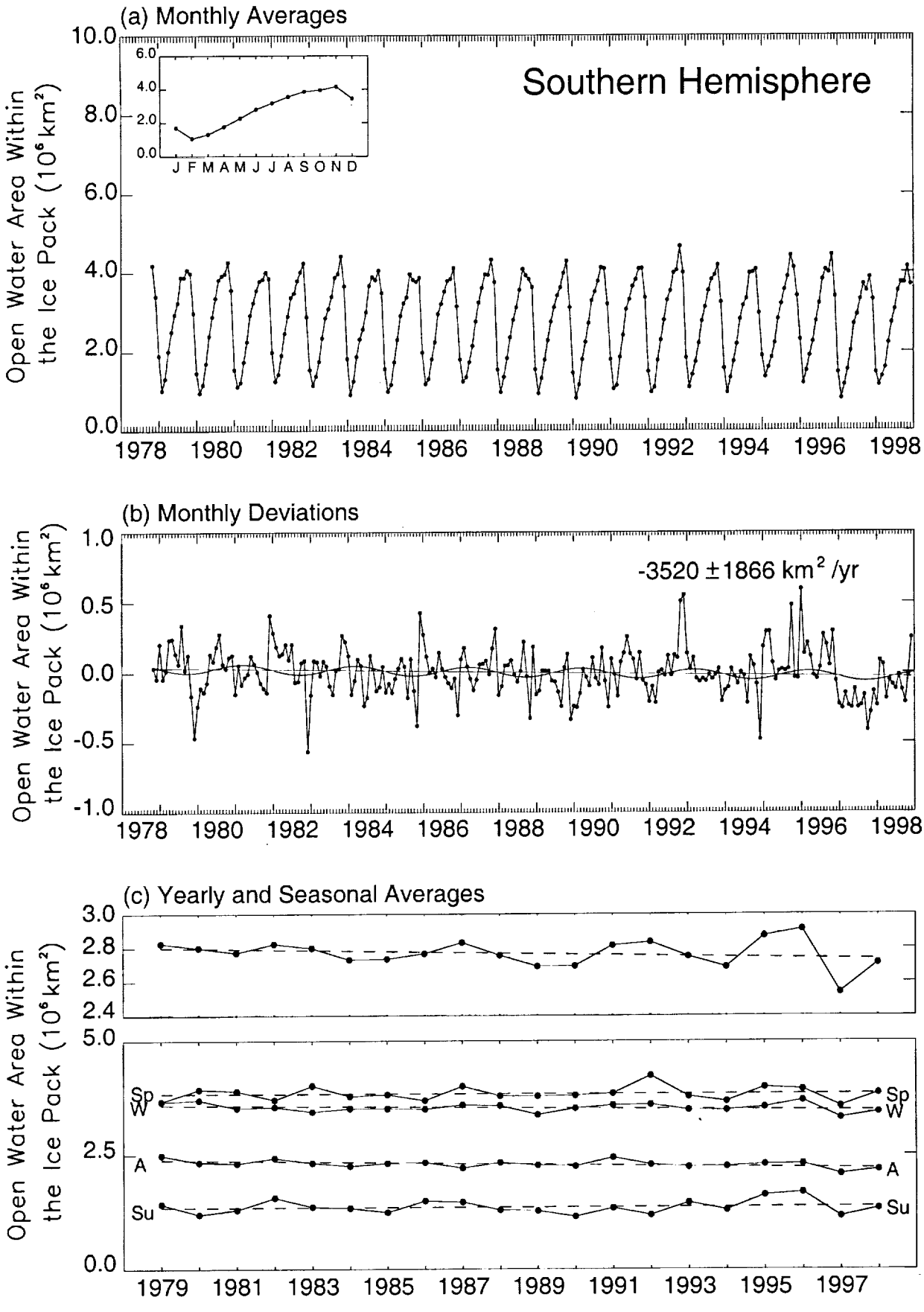
(a) Monthly Averages
Southern Hemisphere
Open Water Area Within the Ice Pack (10^6 km^2)
10.0
8.0
6.0
4.0
2.0
0.0
6.0
4.0
2.0
0.0
J F M A M J J A S O N D
1978 1980 1982 1984 1986 1988 1990 1992 1994 1996 1998
(b) Monthly Deviations
-3520 ±1866 km^2 /yr
Open Water Area Within the Ice Pack (10^6 km^2)
1.0
0.5
0.0
-0.5
-1.0
1978 1980 1982 1984 1986 1988 1990 1992 1994 1996 1998
(c) Yearly and Seasonal Averages
Open Water Area Within the Ice Pack (10^6 km^2)
3.0
2.8
2.6
2.4
5.0
2.5
0.0
Sp
W
A
Su
1979 1981 1983 1985 1987 1989 1991 1993 1995 1997

Figure 14.

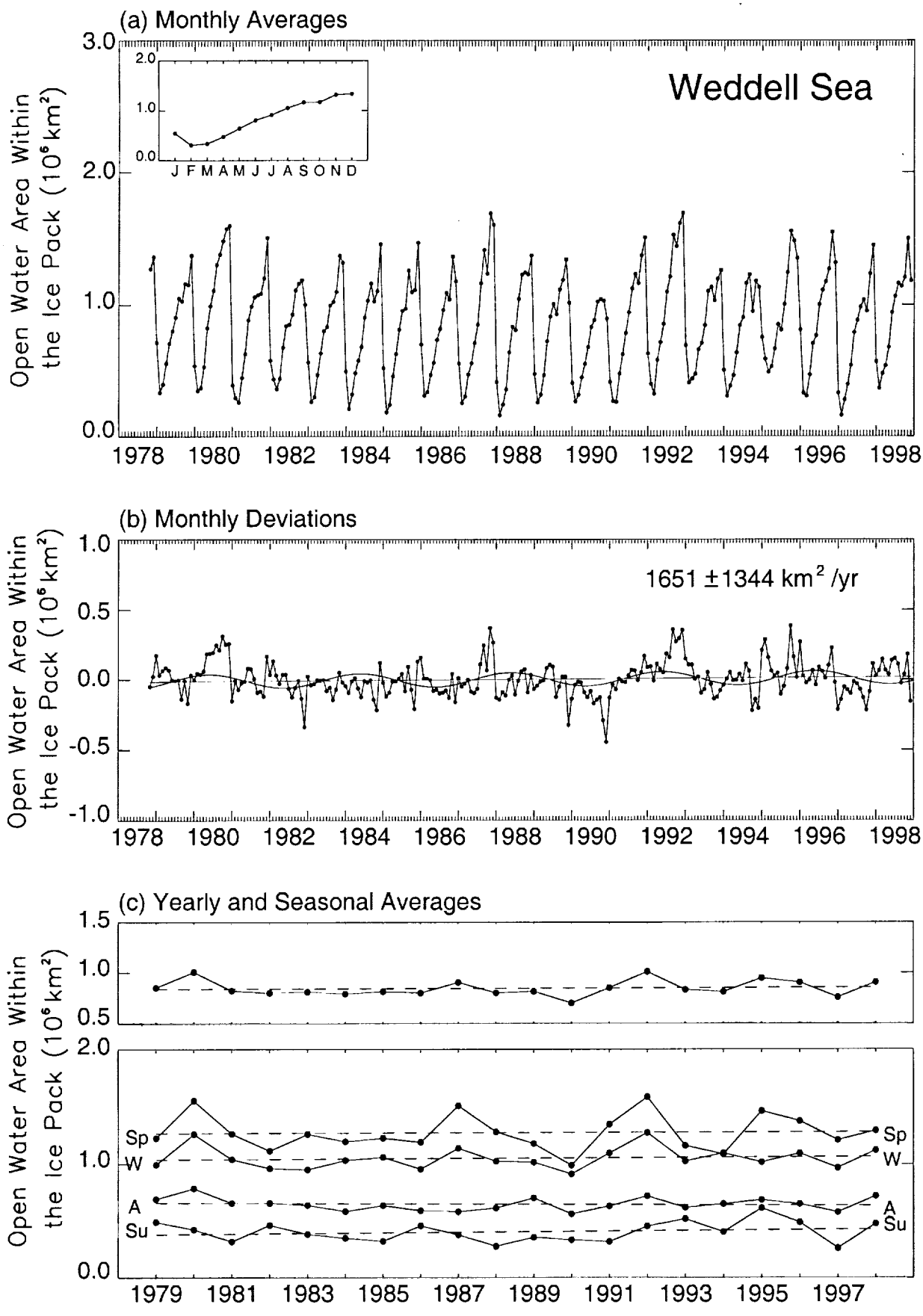
(a) Monthly Averages
Weddell Sea
Open Water Area Within the Ice Pack (10^6 km^2)
3.0
2.0
1.0
0.0
2.0
1.0
0.0
J F M A M J J A S O N D
1978 1980 1982 1984 1986 1988 1990 1992 1994 1996 1998
(b) Monthly Deviations
1651 ±1344 km^2 /yr
1.0
0.5
0.0
-0.5
-1.0
(c) Yearly and Seasonal Averages
1.5
1.0
0.5
2.0
1.0
0.0
Sp
W
A
Su
1979 1981 1983 1985 1987 1989 1991 1993 1995 1997

Figure 15.

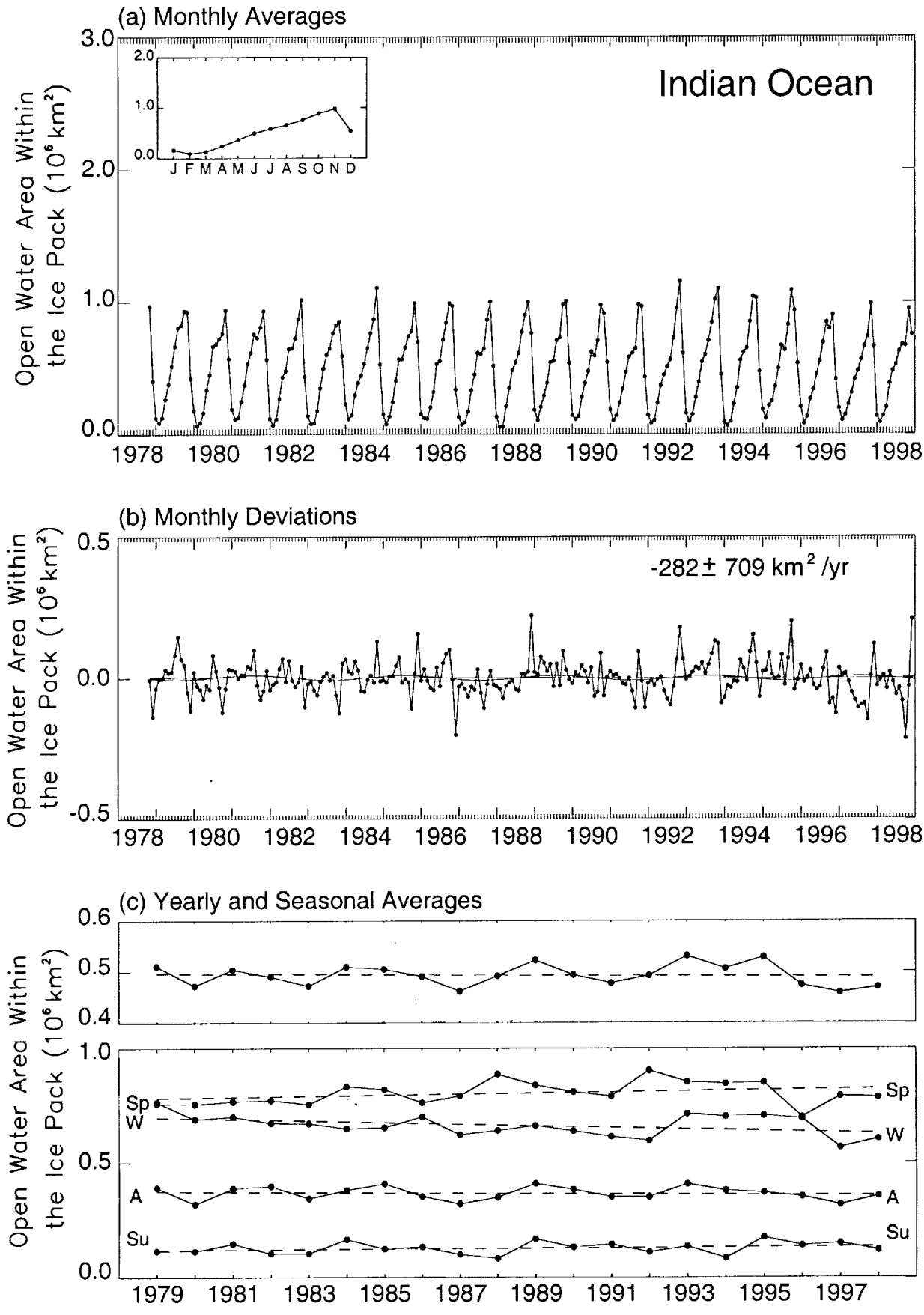
(a) Monthly Averages
Indian Ocean
Open Water Area Within the Ice Pack (10^6 km^2)
3.0
2.0
1.0
0.0
2.0
1.0
0.0
J F M A M J J A S O N D
1978 1980 1982 1984 1986 1988 1990 1992 1994 1996 1998
(b) Monthly Deviations
-282± 709 km^2 /yr
0.5
0.0
-0.5
(c) Yearly and Seasonal Averages
0.6
0.5
0.4
1.0
0.5
0.0
Sp
W
A
Su
1979 1981 1983 1985 1987 1989 1991 1993 1995 1997

Figure 16.

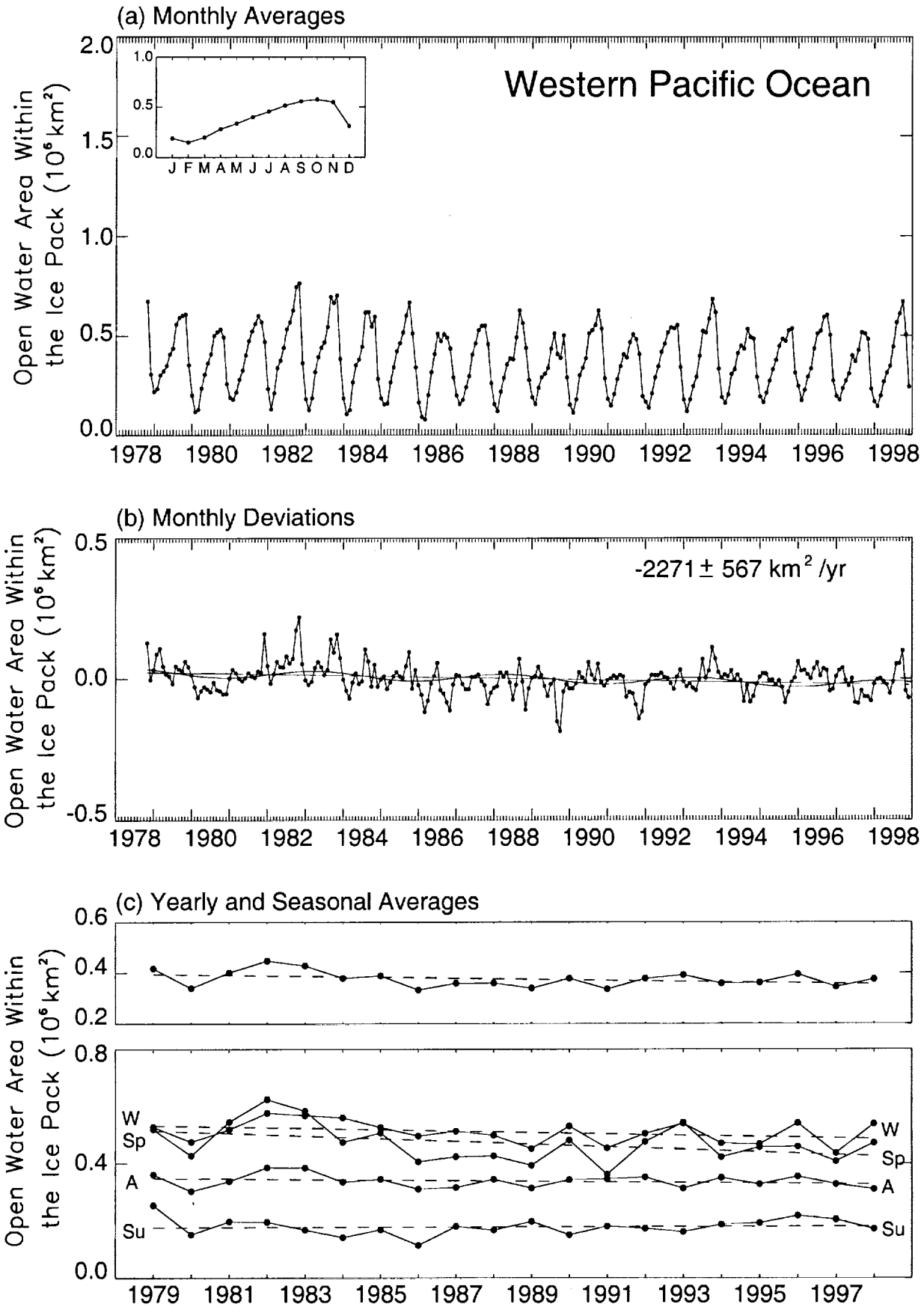
(a) Monthly Averages
Western Pacific Ocean
Open Water Area Within the Ice Pack (10^6 km^2)
2.0
1.5
1.0
0.5
0.0
1.0
0.5
0.0
J F M A M J J A S O N D
1978 1980 1982 1984 1986 1988 1990 1992 1994 1996 1998
(b) Monthly Deviations
-2271 ± 567 km^2 /yr
0.5
0.0
-0.5
1978 1980 1982 1984 1986 1988 1990 1992 1994 1996 1998
(c) Yearly and Seasonal Averages
0.6
0.4
0.2
0.8
0.4
0.0
W
Sp
A
Su
1979 1981 1983 1985 1987 1989 1991 1993 1995 1997

Figure 17

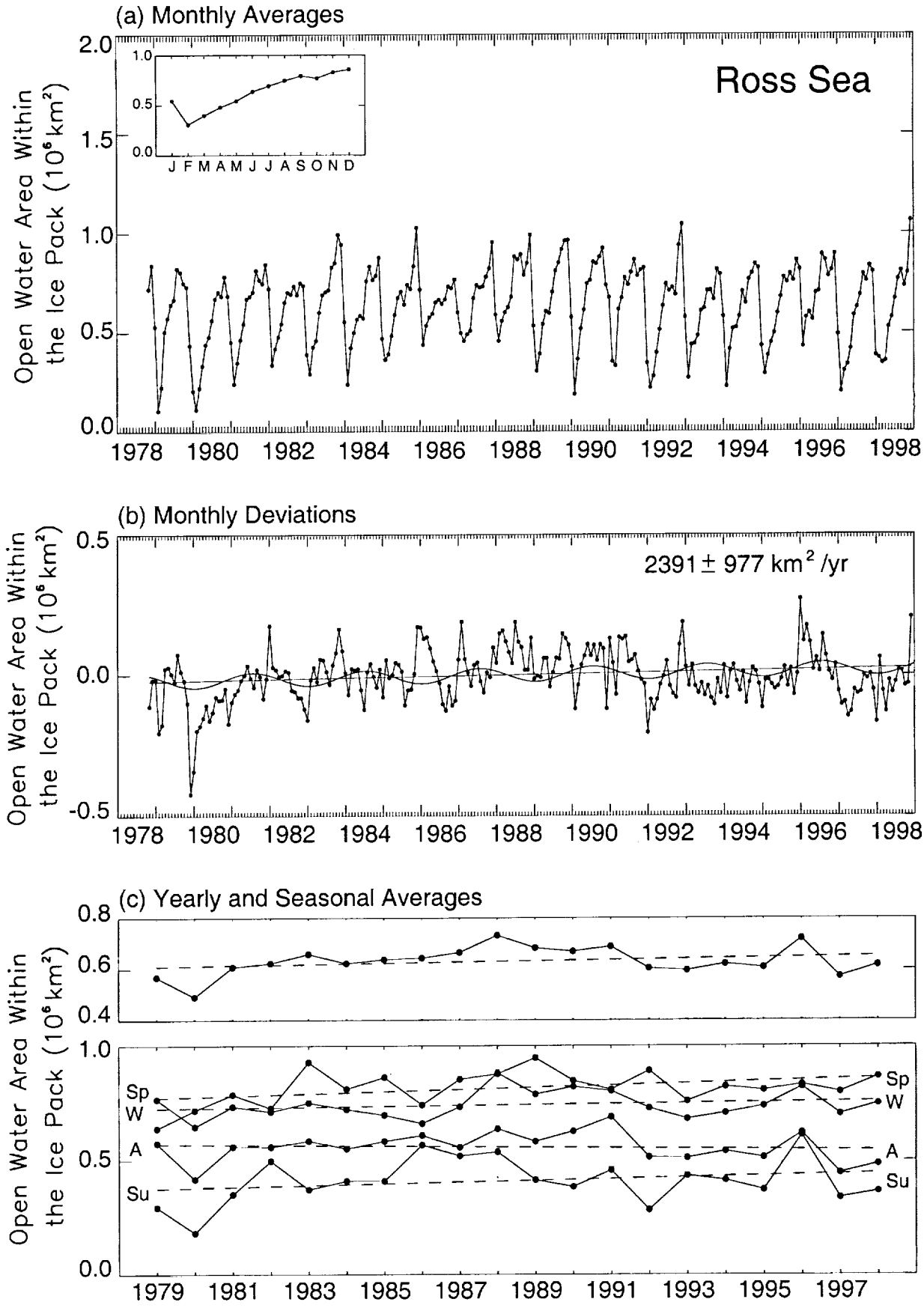
(a) Monthly Averages
Ross Sea
Open Water Area Within the Ice Pack (10^6 km^2)
2.0
1.5
1.0
0.5
0.0
1.0
0.5
0.0
J F M A M J J A S O N D
1978 1980 1982 1984 1986 1988 1990 1992 1994 1996 1998
(b) Monthly Deviations
2391 ± 977 km^2 /yr
0.5
0.0
-0.5
(c) Yearly and Seasonal Averages
0.8
0.6
0.4
1.0
0.5
0.0
Sp
W
A
Su
1979 1981 1983 1985 1987 1989 1991 1993 1995 1997

Figure 18.

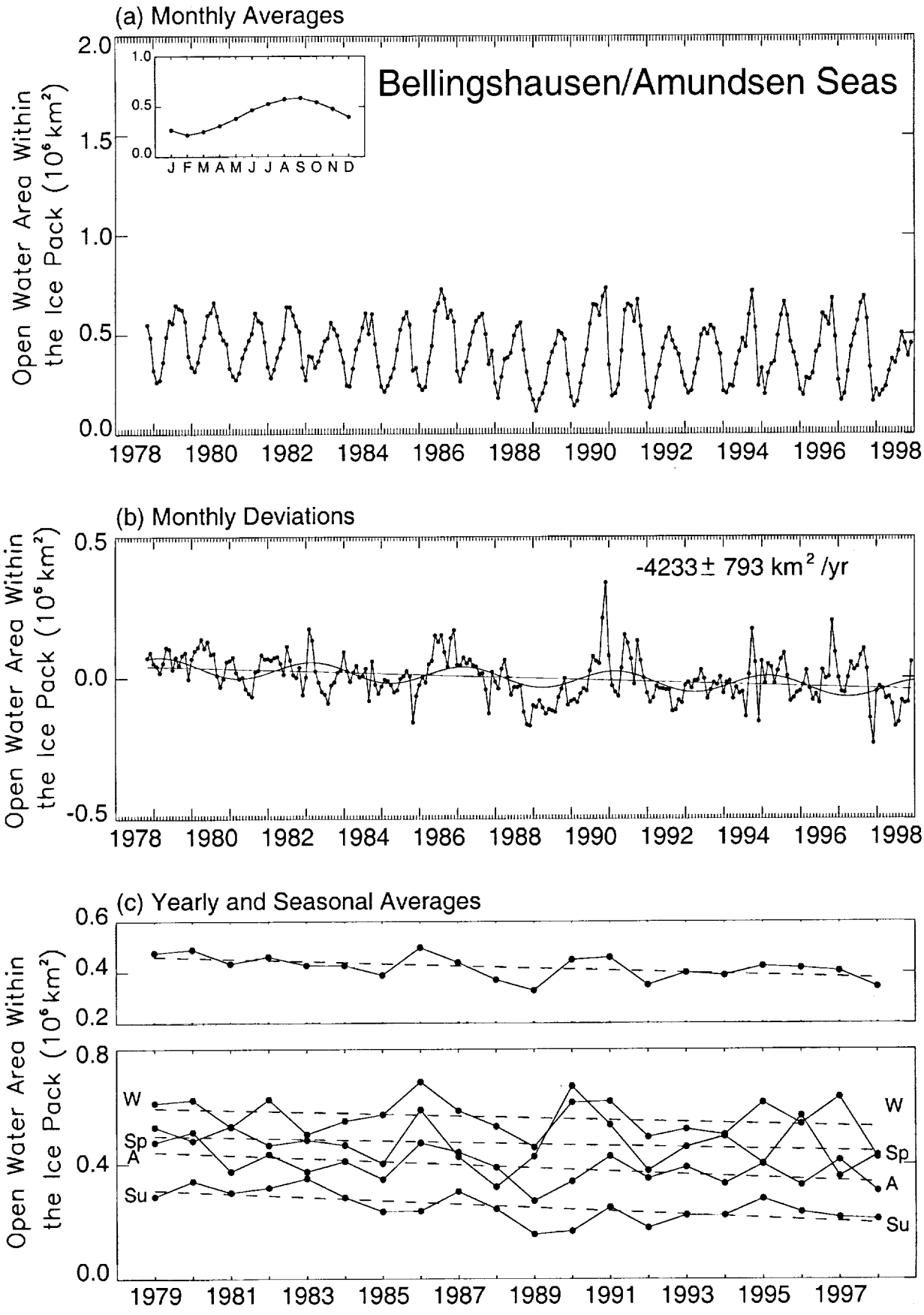
(a) Monthly Averages
Bellingshausen/Amundsen Seas
J F M A M J J A S O N D
Open Water Area Within the Ice Pack (10^6km^2)
(b) Monthly Deviations
-4233± 793 km^2 /yr
(c) Yearly and Seasonal Averages
W
Sp
A
Su
1978 1980 1982 1984 1986 1988 1990 1992 1994 1996 1998
1979 1981 1983 1985 1987 1989 1991 1993 1995 1997

Figure 19.

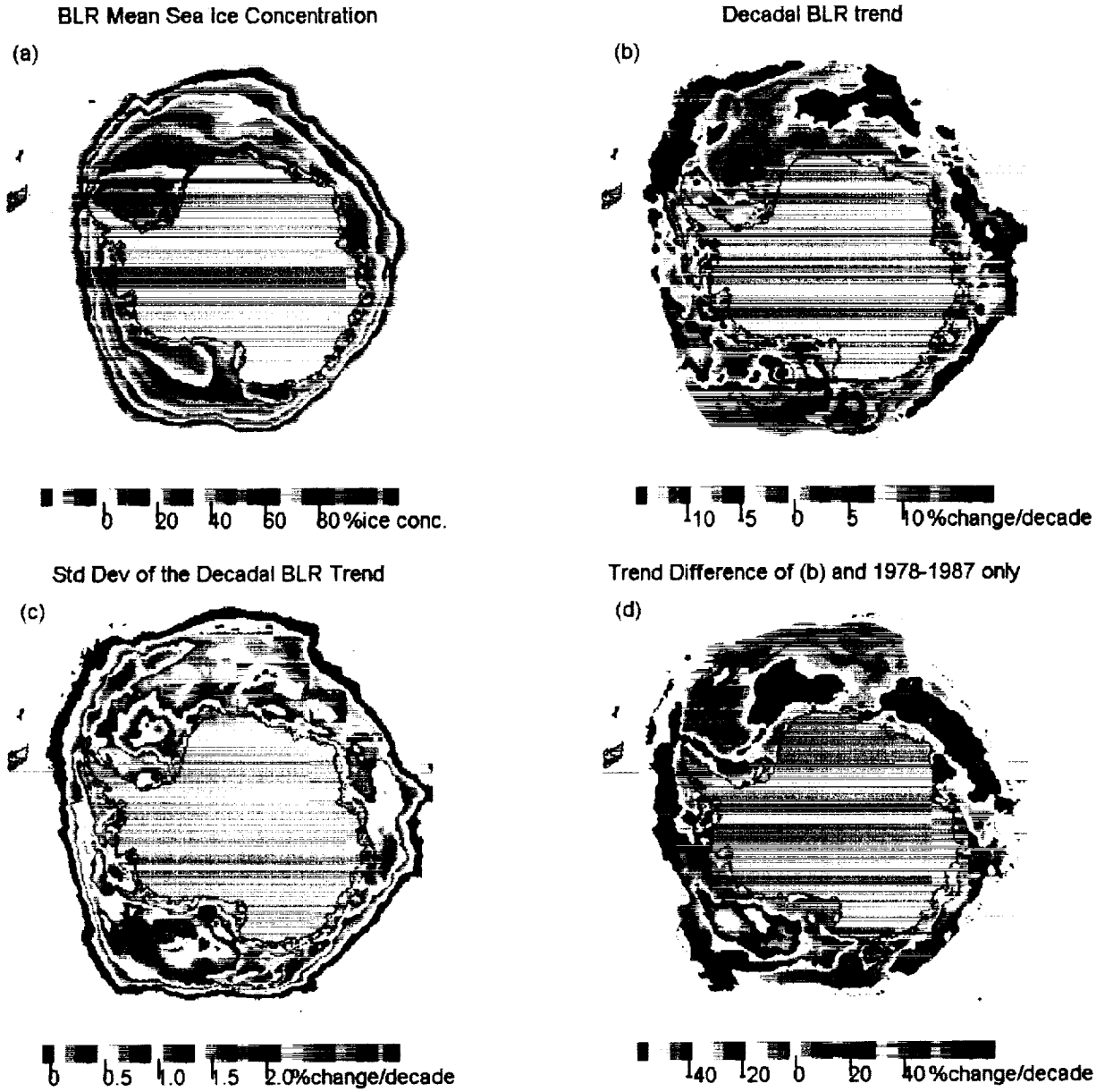
BLR Mean Sea Ice Concentration
(a)
0
20
40
60
80%ice conc.
Decadal BLR trend
(b)
10
5
0
5
10%change/decade
Std Dev of the Decadal BLR Trend
(c)
0
0.5
1.0
1.5
2.0%change/decade
Trend Difference of (b) and 1978-1987 only
(d)
40
20
0
20
40%change/decade

Figure 20

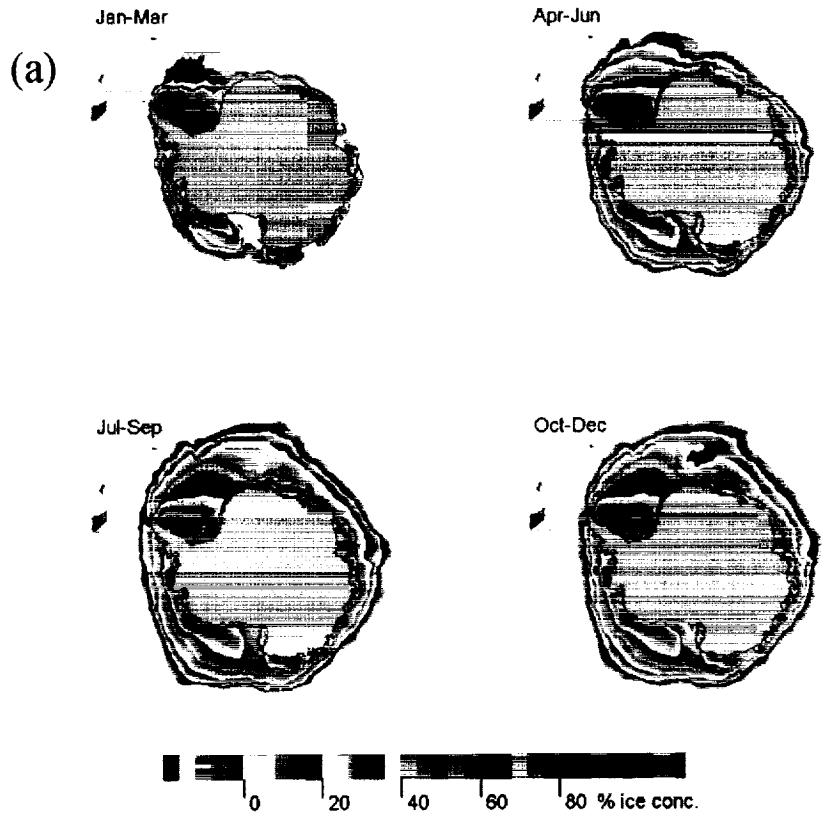
(a)
Jan-Mar
Apr-Jun
Jul-Sep
Oct-Dec
0
20
40
60
80 % ice conc.
(b)
Jan-Mar
Apr-Jun
Jul-Sep
Oct-Dec
-20
-10
0
10
20 % ice conc. change/decade

Figure 21

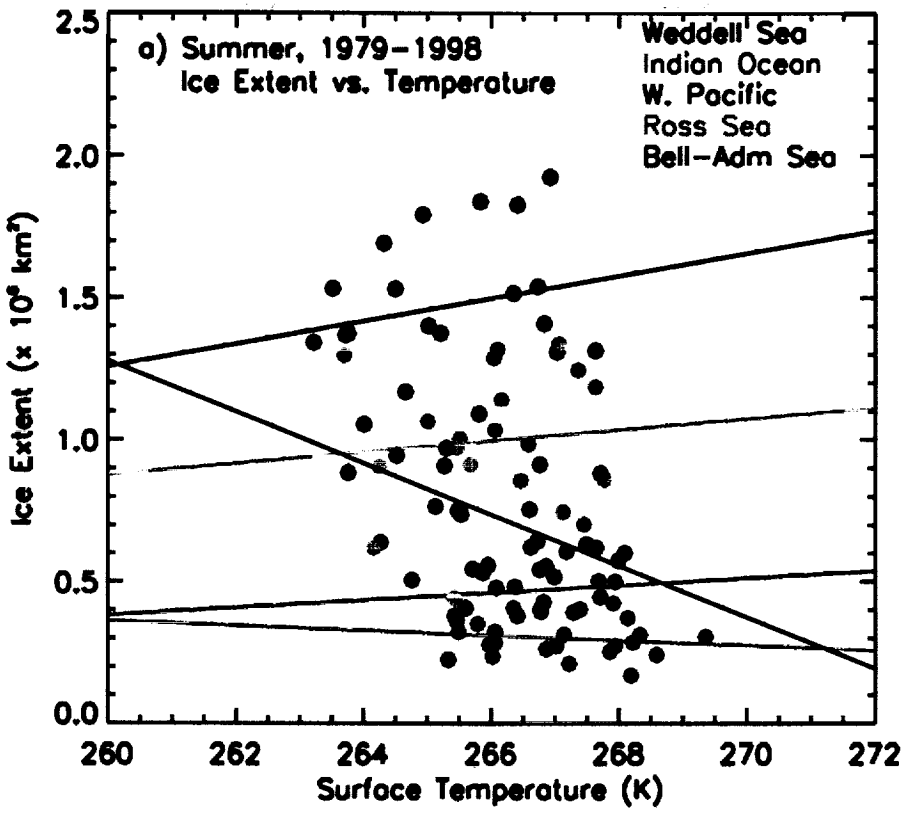
a) Summer, 1979–1998
Ice Extent vs. Temperature
Weddell Sea
Indian Ocean
W. Pacific
Ross Sea
Bell–Adm Sea
Ice Extent (x 10⁶ km²)
Surface Temperature (K)
2.5
2.0
1.5
1.0
0.5
0.0
260
262
264
266
268
270
272

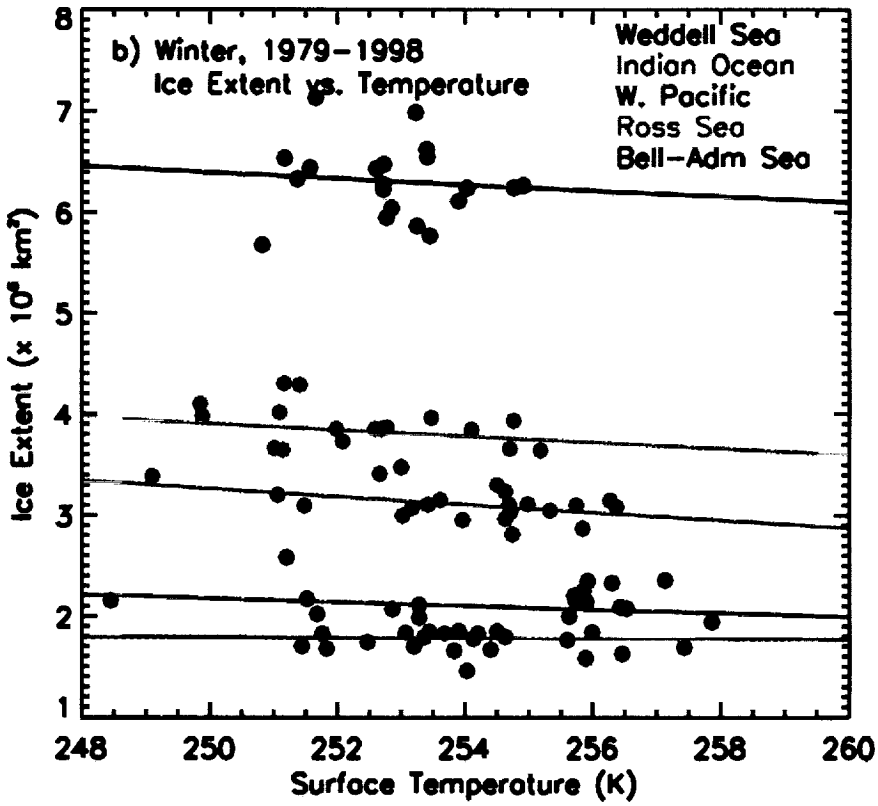
b) Winter, 1979–1998
Ice Extent vs. Temperature
Weddell Sea
Indian Ocean
W. Pacific
Ross Sea
Bell–Adm Sea
Ice Extent (x 10⁶ km²)
Surface Temperature (K)
8
7
6
5
4
3
2
1
248
250
252
254
256
258
260

Figure 22

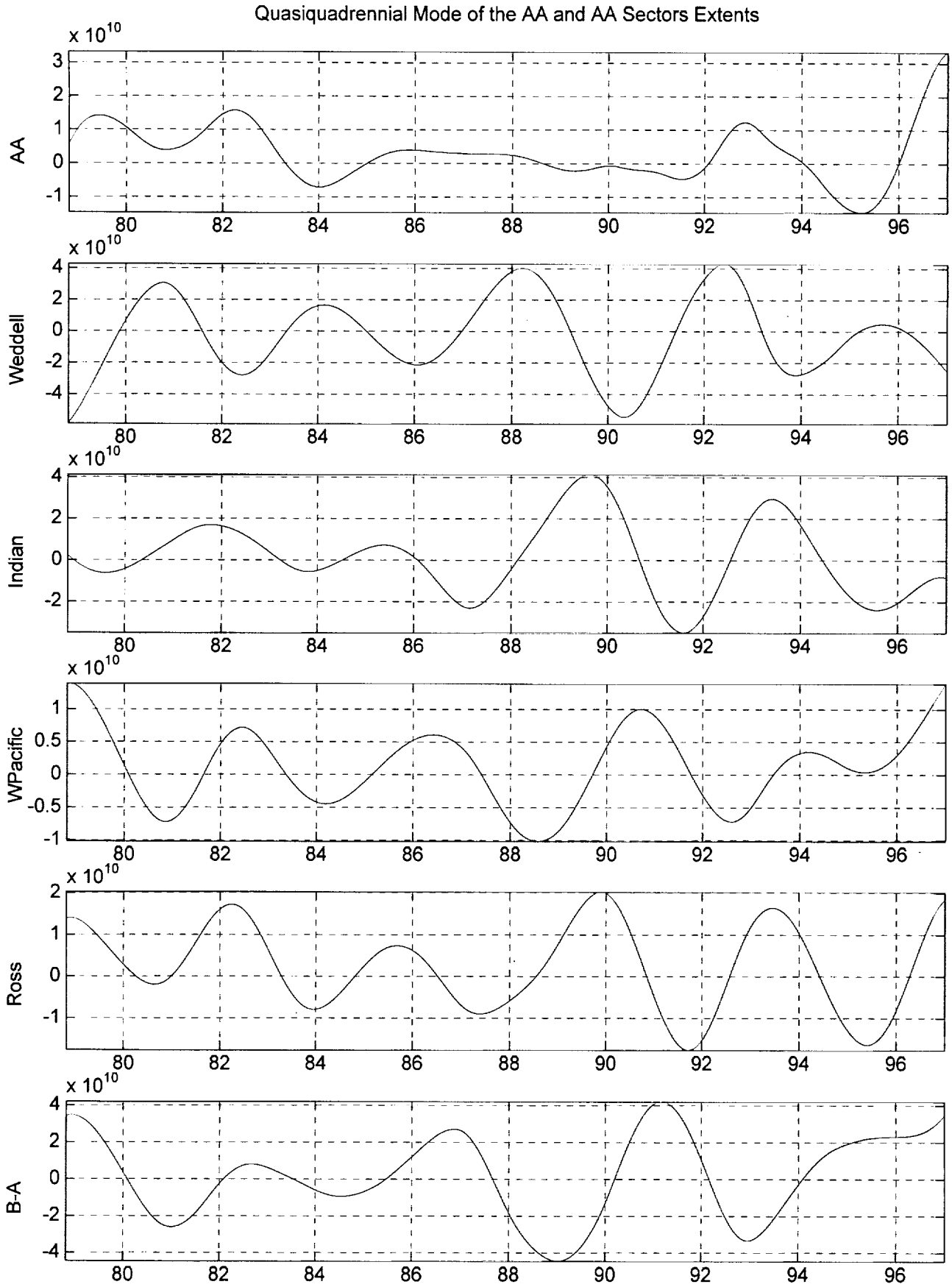
Quasiquadrennial Mode of the AA and AA Sectors Extents
AA
Weddell
Indian
WPacific
Ross
B-A
x 10^10
80
82
84
86
88
90
92
94
96

Figure 23

POPULAR SUMMARY
HJZ, August 16, 2001

Variability of Antarctic Sea Ice 1979-1998

H. Jay Zwally, Josefino C. Comiso, Claire L. Parkinson, Donald J. Cavalieri and Per Gloersen

The total Antarctic sea ice extent (concentration >15%) increased by 13,440 ± 4180 km^2/year (+1.18 ± 0.37%/decade). The area of sea ice within the extent boundary increased by 16,960 ± 3,840 km^2/year (+1.96 ± 0.44%/decade). Regionally, the trends in extent are positive in the Weddell Sea (1.5 ± 0.9%/decade), Pacific Ocean (2.4 ± 1.4%/decade), and Ross (6.9 ± 1.1%/decade) sectors, slightly negative in the Indian Ocean (-1.5 ± 1.8%/decade) and strongly negative in the Bellingshausen-Amundsen Seas sector (-9.5 ± 1.5%/decade). For the entire ice pack, small ice increases occur in all seasons with the largest increase during autumn. Components of interannual variability with periods of about 3 to 5 years are regionally large, but tend to counterbalance each other in the total ice pack. The interannual variability of the annual mean sea-ice extent is only 1.6% overall, compared to 5% to 9% in each of five regional sectors. Analysis of the relation between regional sea ice extents and spatially-averaged surface temperatures over the ice pack gives an overall sensitivity between winter ice cover and temperature of - 0.7% change in sea ice extent per K. The observed increase in Antarctic sea ice cover is counter to the observed decreases in the Arctic. It is also qualitatively consistent with the counterintuitive prediction of a global atmospheric-ocean model of increasing sea ice around Antarctica with climate warming due to the stabilizing effects of increased snowfall on the Southern Ocean.